Geothermics 96 (2021) 102147

Contents lists available at ScienceDirect

Geothermics

journal homepage: www.elsevier.com/locate/geothermics

Lower carboniferous fractured carbonates of the Campine Basin (NE-Belgium) as potential geothermal reservoir: Age and origin of open carbonate veins

Rudy Swennen [a,*], Eva van der Voet [a,b], Wei Wei [a], Philippe Muchez [a]

[a] KU Leuven, Department of Earth & Environmental Sciences, Geology, Celestijnenlaan 200E, B-3001 Heverlee, Belgium
[b] Vlaamse Instelling voor Technologisch Onderzoek (VITO NV), Boeretang 200, B-2400, Mol, Belgium

ARTICLE INFO

Keywords:
Lower Carboniferous
Limestones
U/Pb dating
Clumped isotopes
Open veins
Campine Basin (Belgium)

ABSTRACT

Within the Lower Carboniferous limestones in the boreholes of Poederlee, Heibaart and Turnhout (Campine Basin, NE-Belgium), open veins partially cemented by calcite and dolomite are considered important with regard to the geothermal reservoir potential of these limestones. Based on a detailed petrographic analysis, stable carbon and oxygen as well as clumped Δ_{47} isotope analysis and U/Pb age dating, the formation conditions of these veins have been reconstructed and were placed in the geodynamic evolution of the sedimentary basin. All host rocks are recrystallized, and the open carbonate vein cements often possess a similar depleted $\delta^{18}O_{PDB}$ signature as their recrystallized host rock. The latter thus indicates vein cement precipitation was likely rock-buffered. The $\delta^{13}C$ signature of the host rock often displays a marine signature, while in the veins two isotopic clusters can be differentiated. The first cluster groups veins with cleavage twins, and are characterized by slightly to moderately depleted $\delta^{13}C$, reflecting a mixture of marine carbon with carbon derived from organic matter. This group typically occurs in the open veins from the microbially dominated Poederlee and Heibaart buildups characterised by on-lapping organic-rich Namurian black shales. One of these veins formed at 216 ± 6 °C, indicating that it crystallised during the Sudetic – Asturian deformation stage of late Carboniferous age, while others formed between 110 and 130 °C, indicating that they could have been formed during the late Carboniferous burial stage or after the Sudetic – Asturian deformation and uplift. The second cluster groups veins that may, but often do not, contain cleavage twins. They show host-rock buffered $\delta^{13}C$ signatures. These veins have a Cretaceous (late Aptian/early Albian) and/or Paleocene U/Pb age and formed at temperatures dominantly between 50 and 80 °C based on clumped isotopes.

1. Introduction

In the framework of the global energy transition, the interest in shallow and deep geothermal energy rapidly increased over the last years. The geothermal potential of various reservoirs in the Campine Basin (NE-Belgium; Fig. 1) was first studied by Berckmans and Vandenberghe (1998) and subsequently by Dreesen and Laenen (2010). These authors concluded that the Lower Carboniferous limestone and dolostone sequence possesses a high reservoir potential and likely also a high amount of recoverable heat. First positive indications for encountering good reservoir conditions date back to 1954, when the Lower Carboniferous limestones were studied in the Turnhout borehole (17E225)(Gulinck, 1956). Temperatures up to 80 °C at a depth of about 2200m were reported by Grosjean (1954). However, it lasted till the 1980s before additional efforts were made to evaluate the geothermal potential of the Campine Basin. Firstly, the Meer (07E205IIb) borehole was drilled in 1980-1981, but unfortunately the Lower Carboniferous limestones were not reached. Confirmation of the excellent reservoir characteristics of the Lower Carboniferous limestones were retrieved from the boreholes drilled in the framework of the underground gas storage site in Loenhout (Heibaart structure; Bless et al., 1981; Muchez et al., 1987b; Jaarsma et al., 2013). Subsequently in 1983, the Merksplas (17W265) borehole, situated 6 km from Loenhout, was successfully drilled. Unfortunately, due to the economic situation at that time and the low demand for alternative energy resources, the geothermal project was suspended. Evaluation of the cores by Vandenberghe et al. (2000)

* Corresponding author.
E-mail address: Swennen@kuleuven.be (R. Swennen).

https://doi.org/10.1016/j.geothermics.2021.102147
Received 26 January 2021; Received in revised form 30 April 2021; Accepted 17 May 2021
Available online 6 June 2021

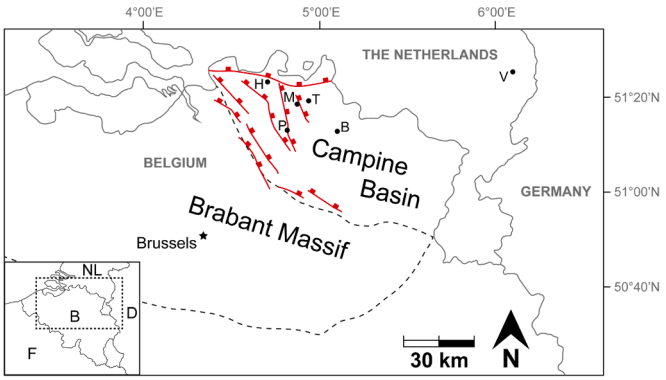

Fig. 1. Geographical position of the Heibaart (H), Poederlee (P) and Turnhout (T) boreholes as well as other locations referred in the text (M = Merksplas; B = Balmatt; V = Venlo). The faults (in red) are redrawn from Muchez and Langenaeker (1993). (For interpretation of the references to color in this figure legend, the reader is referred to the web version of this article.)

with regard to reservoir permeability, temperature and brine composition were in line with the observations made in the Turnhout borehole. But as reported by Kombrink (2008) and Van Hulten and Poty (2008) only limited borehole control exists in the southern Netherlands and northern Belgium and most of the boreholes are clustered around the margins of the Carboniferous basin. In addition, seismic coverage is poor because most seismic data were acquired and processed with a focus on the younger, shallower formations that locally have hydrocarbon potential (Van Hulten and Poty, 2008). Recent projects were carried out in the Netherlands (the so-called CWG and CLG geothermal boreholes CAL-GT-01, 03, 04 & 05 near Venlo) (Jaarsma et al., 2013; Reith et al., 2019). Here the reservoir is to some extent characterized by hypogene karstification (Poty, 2014). The Balmatt project in northern Belgium near Mol is another geothermal project (Bos and Laenen, 2017; Broothaers et al., 2019). Unfortunately, the latter two projects were jeopardized by minor induced earthquakes due to the reinjection of water in the subsurface. Recently, Janssen Pharmaceutica have drilled a doublet targeting the Lower Carboniferous carbonates at Beerse (northern Belgium). For a comprehensive overview of the state of art of the Lower Carboniferous carbonates in the southern Netherlands and northern Belgium the reader is advised to consult Reijmer et al. (2017).

The Lower Carboniferous dolostone and limestone succession is the main target for deep geothermal energy, despite the fact that these lithologies display low matrix porosities. In such systems, the existence of open fractures is of major importance (Warren and Root, 1963; Nelson, 1985). In the case of the Campine Basin the latter have also been affected by a late Viséan to early Namurian karstification (Vandenberghe and Bouckaert, 1980; Dreesen et al., 1987) and locally hypogene karstification during burial (Muchez et al., 1991a; Poty, 2014). Consequently, a profound knowledge of the fracture networks is needed (Van der Voet et al., 2020a, 2020b; Van der Voet et al., in preparation). However, to be able to unravel the evolution of fracturing and especially of the subsequent partial cementation of the fractures, the precipitation temperature of the fracture-filling cement, the type of ambient fluid involved and if possible some absolute age dating of cements are needed. Recent development of clumped isotope analysis and U/Pb age dating allow to acquire these essential data.

The aim of this paper is to unravel the formation conditions of the partially cemented veins in the Viséan limestones in the Campine Basin. Therefore, cores with partially cemented veins were studied in the Poederlee, Heibaart (DZH1) and Turnhout boreholes (Fig. 1). They were characterized from a petrographical point of view, whereby their cathodoluminescence characteristics are of primordial importance. The stable carbon and oxygen isotope composition, as well as the clumped isotope composition of the carbonate cements yield information on the ambient fluids and the precipitation temperatures. Finally, some vein cements could be dated by applying the U/Pb age dating method allowing to further constrain the time period these veins formed.

The outcome of this study shows that integration of different new analytical techniques allows to better constrain the origin of cement phases in open veins, i.e. whether for example hypogene karstification or meteoric fluids were involved. Based on the age dating of partially cemented veins, an assessment of the stress field that created these veins can be made. Based on the vein orientation it can also be predicted which veins likely will be closed. This helps to set up a strategy for optimal planning if for example deviated boreholes are drilled. This study can serve as a kind of workflow for studying other potential geothermal limestone reservoirs.

2. Geological setting

The three boreholes studied are all situated in the Campine Basin, which is part of the Northwest European Carboniferous Basin (NWECB, Kombrink, 2008). During the early Carboniferous, dominantly shallow marine carbonates were deposited in this area south of the approximately W-E trending Hoogstraten growth fault in the northern part of Belgium. Muchez et al. (1987a) divided the Campine Basin into an eastern and western part based on borehole observations with a synsedimentary fault between the Poederlee-Heibaart reef mounds in the western part and the Turnhout area in the eastern part.

Reef mounds developed near the margin of the shelf at Heibaart (Muchez et al., 1987a, b) and in the shelf interior at Poederlee (Muchez et al., 1990). The block-faulted Campine Basin corresponds to a Variscan foreland basin with a NW-SE axis. The latter stretches from the northern border of the London-Brabant Massif northeastward up to the (Zandvoort-) Maasbommel-Krefeld High complex in the Netherlands and Germany (Bless et al., 1983; Harings, 2014). The large differences in thicknesses of the Viséan limestones are interpreted to relate to block faulting, which are dominated by syn-sedimentary (N)NW-(S)SE trending normal faults (Fig. 1; Bless et al., 1981; Muchez and Langenaeker, 1993; Langenaeker, 2000; Laenen et al., 2004; McCann, 2008; Bos and Laenen, 2017). The Lower Carboniferous carbonates are covered by clastic sediments, that generally show an on-lapping relationship, very well expressed adjacent to the mound carbonates in Poederlee and Heibaart. This geometry points towards the presence of a paleo-relief of the Dinantian carbonates during deposition of the overlying strata. Of importance is also, as mentioned before, that the carbonates display karstic features, related to an emergence period at the end of the Viséan (Reijmer et al., 2017).

The sedimentary succession is generally tilted towards the north-northeast. This tilting relates to the uplift of the London-Brabant Massif in relation to the Kimmerian orogeny (Langenaeker, 2000). As a consequence, the Viséan subcrop deepens towards the north-northeast. The limestones are crossed by WNW-ESE oriented faults (Fig. 1; Muchez and Langenaeker, 1993; Langenaeker, 2000; Laenen et al., 2004). Most of these faults existed already during the Carboniferous (Muchez et al., 1987a). Many of them were subsequently reactivated during the Late Jurassic extensional Cimmerian phase, related to the opening of the Atlantic, and/or during the Late Cretaceous – Early Tertiary Sub-Hercynian and Laramide inversion phase, related to the Alpine collision (Ziegler, 1990; Langenaeker, 2000; Laenen et al., 2004). This was followed by the subsidence of the Roer Valley Graben, east of the Campine Basin (Van Wijhe 1987; Langenaeker, 2000).

3. Methodology

3.1. Petrography

The main aim of the petrographical analysis was to differentiate diagenetic phases and to establish, if possible, a paragenetic sequence of the vein cementing phases. The latter mainly relies on cross-cutting relationships, but based on the limited size of the cores, cross-cutting

relationships are not always present. The petrographical analysis was not to study the host rock constituents, but to assess the potential recrystallization of the host rocks to be able to better interpret the host rock stable isotopic composition. The study is executed with an Olympus BX60 and a Leica DM LP microscope, both using transmitted and polarized light. The latter is connected with a digital DP200 camera and together with the computer software DeltaPix, digital images can be acquired. Scale-bars are added to the images with Axiovision LE (version 4.3). Cathodoluminescence microscopy aims to refine the cement characteristics and where cross-cutting relationships exist, to determine the paragenesis. The used cold cathodoluminescence equipment consisted of a modified Techosyn Model 8200 Mark II.

3.2. Stable carbon and oxygen isotopes

Powdered samples for stable C- and O-isotope analyses were drilled using a hand drill. All samples were analyzed at the 'Friedrich-Alexander-Universität' (Erlangen-Nürnberg, Germany), under the supervision of Prof. dr. Michael Joachimski. Carbonate powders reacted with 100% phosphoric acid at 70 °C using a Gasbench II connected to a ThermoFinnigan Five Plus masspectrometer. All values are reported in per mil, relative to V-PDB by assigning a $\delta^{13}C$ value of +1.95‰ and a $\delta^{18}O$ value of -2.20‰ to the NBS19 standard. The analytical standard deviation for $\delta^{13}C$ is 0.04‰, for $\delta^{18}O$ it is 0.05‰ for the matrix samples. For the cement samples the analytical standard deviation is both for $\delta^{13}C$ and $\delta^{18}O$ is 0.03‰. The results are given in supplementary data 1.

3.3. Clumped isotopes

Powdered samples for clumped isotope analyses were drilled using the same hand drill. The measurements were performed under supervision of Dr. László Rinyu at the Isotoptch Zrt. Institute in Debrecen (Hungary) using a Thermo Scientfic Kiel IV automatic carbonate device coupled to a Thermo Scientific MAT253 Plus isotope ratio mass spectrometer. Each sample consisted of 10-12 replicate analysis of 100μg aliquots. ETH1, ETH2 and ETH3 were used as normalization standards and IAEA-C2 was used as quality control sample with the values reported by Bernasconi et al. (2018). Several of the latter reference samples were also included in the recent study by Bernasconi et al. (2020) in an attempt to improve repeatability across laboratories. For temperature calculation the recalculated Kele calibration was used according to the recommendation of the latter authors:

$$\Delta_{47} = 0.0449(\pm 0.001) \times \left(10^6 / T^2\right) + 0.167(\pm 0.01)$$

where T is the temperature in Kelvin and Δ_{47} is given on a CDES (carbon-dioxide equivalent scale). Data evaluation was carried out with Easotope application (John and Bowen, 2016) using the CO_2 clumped ETH PBL replicate analyses method and Brand parameters. The results are given in Table 1.

3.4. U–Pb age dating of calcite

The applied method was similar to that previously described by Ring and Gerdes (2016) and Burisch et al. (2017). U–Pb ages were acquired in situ from 8 polished thick sections (100–150 μm thick) from core samples containing open calcite cemented veins by laser ablation-inductively coupled plasma-mass spectrometry (LA-ICP-MS) at the Goethe University Frankfurt, under supervision of Dr. Axel Gerdes, using a modified method described in Gerdes and Zeh (2006, 2009). A ThermoScientific Element 2 sector field ICP-MS was coupled to a Resolution S-155 (Resonetics) 193 nm ArF excimer laser (CompexPro 102) equipped with a two-volume ablation cell (Laurin Technic). Samples were ablated in a helium atmosphere (0.4 L min^{-1}) and mixed in the ablation funnel with 0.9 L min^{-1} argon and 0.05 L min^{-1} nitrogen. Signal strength at the ICP-MS was tuned for maximum sensitivity while keeping oxide formation (monitored as $^{248}ThO/^{232}Th$) below 0.2% and no fractionation of the Th/U ratio. Static ablation used a spot size of about 215 μm and a fluence of about 1 J cm^{-2} at 8 Hz. This yielded for the NIST SRM-614 a depth penetration of ~0.6 μms^{-1} and an average sensitivity of 350,000 c/s μg^{-1} for ^{238}U. The detection limit for ^{206}Pb and ^{238}U was ~0.2 and ~0.03 ppb, respectively. Data were acquired in fully automated mode overnight in different sequences. Each analysis consists of 20 s background acquisition followed by 20 s of sample ablation and 25 s washout. During 40 s of data acquisition, the signal of ^{206}Pb, ^{207}Pb, ^{208}Pb, ^{232}Th and ^{238}U were detected by peak jumping in pulse counting mode with a total integration time of 0.1 s, resulting in 420 mass scans. Prior to analysis each spot was pre-ablated for 3 s to remove surface contamination. Soda-lime glass NIST SRM-614 was used as a reference glass together with two carbonate standards to bracket sample analysis. Raw data were corrected offline using an in-house MS Excel© spreadsheet program (Gerdes and Zeh, 2006, 2009). Following background correction, outliers (±2σ) were rejected based on the time-resolved $^{207}Pb/^{206}Pb$ and $^{206}Pb/^{238}U$ ratios. The mean $^{207}Pb/^{206}Pb$ ratio of each analysis was corrected for mass bias 0.3% and the $^{206}Pb/^{238}U$ ratio for inter-element fractionation (~5%), including drift over the sequence time, using NIST SRM-614. The $^{206}Pb/^{238}U$ fractionation during 20s depth profiling was estimated to be 3%, based on the common Pb corrected WC-1 analyses, and has been applied as an external correction to all carbonate analyses. Repeated analyses of a Zechstein dolomite (Gypsum pit, Tettenborn, Germany) as well as a stromatolitic limestone from the Cambrian-Precambrian boundary from South-Namibia were carried out as secondary (in-house) standards. Altogether the data imply an accuracy and repeatability of the method of ~2% or better. Data were plotted in Tera-Wasserburg diagrams and ages calculated as lower intercepts using Isoplot 3.71 (Ludwig, 2009). All uncertainties are reported at the 2σ level.

Table 1
Results of stable C- and O-isotopes and Δ_{47} clumped isotopes as well as calculated temperatures of different samples with specific vein types (i.e. open dolomite (TU20) and calcite vein infills (all other data)). For information on vein types see text.

Sample/vein type	$\delta^{13}C$ [‰]		$\delta^{18}O$[‰] vPDB		$\delta^{18}O$[‰] vSMOW	$\delta^{18}O$[‰] vSMOW	Δ_{47} [CDES25]		Kele Temp [°C]	± SE °C
	Value	SD	Value	SD	carbonate	water	Value	SD		
PO15C/PC2	1.06	0.06	-12.26	0.10	18.29	4.7	0.454	0.029	122	6
PO15I/PC2	1.46	0.05	-11.58	0.11	19.12	6.3	0.445	0.019	129	4
PO20/PC4	-0.03	0.10	-8.01	0.13	22.68	1.4	0.558	0.033	66	4
HE22/HC7	1.20	0.04	-11.68	0.08	18.87	-5.3	0.602	0.049	48	6
HE24O/HC7	1.14	0.05	-11.83	0.09	18.71	-4.9	0.595	0.047	51	4
HE24V/HC4	-0.76	0.09	-13.32	0.08	17.25	3.9	0.452	0.017	124	4
HE25/HC3 or 5	1.07	0.06	-11.62	0.08	18.94	1.2	0.509	0.030	89	5
HE28/HC3	0.57	0.09	-8.60	0.22	22.05	0.2	0.567	0.027	62	3
TU20B/TD1	2.38	0.04	-12.81	0.08	17.75	-5.2	0.531	0.049	78	8
TU20S/TD1	2.48	0.04	-13.12	0.11	17.28	-5.5	0.527	0.053	80	9
TU23/TC1	1.47	0.04	-14.82	0.08	15.65	0.5	0.475	0.023	109	4
TU25/TC2B	2.30	0.04	-8.83	0.09	21.80	17.0	0.355	0.016	216	6

4. Results

The acquired results will be first presented for the different boreholes separately, starting with the results from Poederlee, followed by Heibaart and Turnhout, before a synthesis is given. Examples of open veins are given in Fig. 2.

4.1. Stratigraphy and sedimentology

The 168 m thick Viséan strata encountered in the Poederlee borehole (1689 – 1521 m) belong to the upper part of the Lower Warnantian (Muchez et al., 1990). They make up a domal structure, inferred from the inclined nature of the beds versus some geopetal infill. The succession is characterized by 5 sedimentary cycles, of which the thickness varies between 13 and 45 m, with decreasing unit thickness upwards. In the lower part of each unit fossil-rich mudstones, bioclast-rich wackestones, peloidal packstones and cryptalgal boundstones often with fibrous or radiaxial cements dominate. These reflect reef mound structures. In the upper part bioclast-rich wacke-, pack- and grainstones occur which reflect shallow open marine depositional conditions.

In the Heibaart DZH1 borehole, the Viséan has a thickness of 297 m (1399 – 1102 m) (Muchez et al., 1987a). It reaches the Upper Moliniacian (Lower Viséan). Nearly no Lower Moliniacian strata were deposited in this area, as inferred from the nearby TOTAL borehole Heibaart 1+1bis, likely because this area acted as a high during this stage (Muchez et al., 1987b). The 112 m thick Upper Moliniacian with mainly bioclast-rich wacke- till grainstone, with an open marine fauna, is often intensively recrystallized. These strata are indicative for subtidal sedimentation conditions. The 43 m thick Livian (Middle Viséan) bioclast-rich wacke- to packstones reflect shallow open marine sedimentation conditions, deposited mostly below wave base (Muchez et al., 1987a). In the Lower Warnantian (Upper Viséan), two units can be differentiated. The lower unit (1244 – 1225 m) with lithoclast-rich and bioclast-rich wacke-, pack- and grainstones with open marine fauna was deposited near wave base. The strata in the upper unit (1225 – 1102 m) are mainly composed of cryptalgal lithologies with stromatactis-like cavities filled by fibrous and radiaxial cements (Muchez et al., 1991b). The latter features are indicative for reef mound structures with sedimentation below wave base evolving to shallower sedimentation conditions as inferred from its fossil content (Muchez et al., 1987a).

The Dinantian succession in the Turnhout borehole is 544 m thick (2706 – 2162 m), however, the base of the Viséan was not reached (Muchez et al., 1987b). In the Lower Moliniacian (Lower Viséan), which is 423 m thick, two main lithological units can be differentiated. In the lower unit (2706 – 2550 m) dominantly peloidal boundstones with fenestrae containing blue-green (Schyzophyta) and green algae (Chlorophyta) occur. These cryptalgal limestones are interpreted as dominantly intertidal deposits. The upper bioclast-rich peloidal pack- to grainstones (2550 – 2282 m) with algal lumps, faecal pellets and coated grains are interpreted as subtidal deposits whereby the algal lumps point towards a protected depositional setting. The Upper Moliniacian (Lower Viséan) is only 12 m thick and consists of bioclast-rich packstone indicative for below wave-base sedimentation. Subsequently (2270-2258 m) peloidal mudstone with fenestrae and radiaxial cements forming a small cryptalgal mound follow, upon which bioclast-rich pack-, grain- and rudstones were deposited which are intensively recrystallized. The latter are interpreted as mound flank facies. The overlying 53 m thick Lower Warnantian (Upper Viséan) consists of lithoclast- and bioclast-rich rudstones (micro breccias), peloidal mudstones (boundstones) indicative for mound structures and bioclast-rich wacke-, pack- and grainstones interpreted as mound flank facies. The upper part is heavily silicified. The overlying Upper Warnantian (Upper Viséan) consists of intense diagenetically altered lithologies.

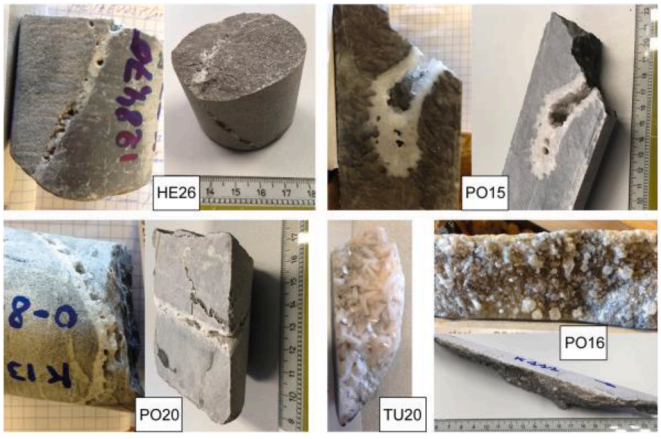

Fig. 2. Illustration of cores (with used numbering in this study) with open veins or partially calcite cemented cavities, with the exception of sample TU20 (lower left picture) which consists of saddle dolomite (HE26 and PO20 are 5 cm in diameter; PO15 is 6.5 cm in diameter; TU20 and PO16 are cut pieces with 2 cm in diameter).

4.2. Diagenesis of the open veins

Note that the diagenetic history presented below focusses on open veins and associated cemented veins, which not necessarily are representative for the entire diagenetic history of the Dinantian succession in the studied boreholes. The studies of Muchez et al. (1991a, b, 1994a, b) focussed on the diagenetic evolution of the cements and veins, but not on the open or partially cemented fractures, i.e. the open veins. The latter fractures, however, determine the current reservoir characteristics of the Upper Viséan strata (Van der Voet et al., 2020a). In the sections below we first will address some diagenetic features within the host rocks adjacent to the open veins, which are followed by the description of the veins, based on which subsequently a brief interpretation is added for each borehole. With regard to the veins in the Poederlee borehole a consistent paragenesis could be worked out based on cross-cutting relationships. This, unfortunately was not possible for the Heibaart and Turnhout boreholes, due to the absence of sufficient number of cross-cutting partly cemented veins. However, based on the cross-cutting relationships the partly cemented veins formed after the latest completely cemented vein generation, i.e. the dolomite cemented veins formed at 200 °C during maximum burial (Muchez et al., 1991a).

The main lithology in the studied Poederlee samples consists of neomorphosed mud- to wackestone. The neomorphic nature is supported not only by the obliteration of primary textures but also by the locally bright blotchy luminescence of the matrix. Elongated authigenic quartz crystals with faint zoning and up to 1cm in length frequently occur. Locally some of these quartz crystals float into calcite veins. Primary pores and cavities are bordered by impure skalenohedral first dull luminescent and then orange zoned calcite which becomes more transparent and coarse crystalline towards the centre of the pores (Fig. 3A).

The first vein infill in the Poederlee samples, that only locally developed, consists of thin bright orange luminescent cement, often with irregular outline (PC1)(Fig. 3C). The latter macroscopically correspond to white non-ferroan completely cemented calcite veins. They are crosscut by macroscopically white closed, slightly ferroan calcite veins, possessing a uniform to broadly zoned dull luminescence (PC2) (Fig. 3C) and with well-developed cleavage twins. Locally some dull luminescent dolomite phases (PD1) occur within PC2 (Fig. 3D). They are crosscut by bed-parallel stylolites. In most samples the third open vein generation, cross-cutting and overgrowing but locally also recrystallising the former cement phases consists of a zoned orange calcite (PC3) (Fig. 3B, C & D), that macroscopically has a white colour. The zonation pattern is, however, not uniform all over the studied samples. Cleavage twins only seldom occur in this cement. Upon the latter some pyrite crystals occur.

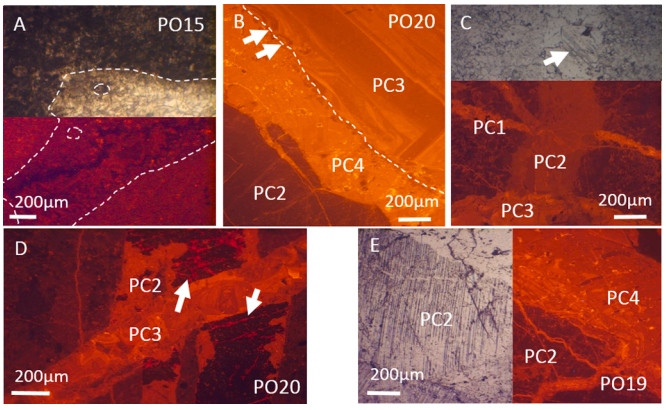

Fig. 3. Representative illustrations of diagenetic features in the Poederlee borehole (coloured parts are taken under cathodoluminescence while grey parts are taken under transmitted light microscopy). A. Primary pore bordered by impure skalenohedral first dull luminescent and then orange zoned calcite which becomes more transparent and coarser crystalline towards the centre of the pores. B. Vein filled with first dull luminescent calcite PC2, followed by zoned orange calcite PC3 (notice the growth zoning upon the irregular border; see arrows), which became detached from PC2. Along this detachment a more brightly zoned orange calcite PC4 developed in the reactivated fracture. C. Irregular thin bright orange luminescent calcite veinlets (PC1), cut by a broadly zoned dull luminescent calcite (PC2) with cleavage twins (see arrow), which on its turn is cut by a zoned orange calcite PC3 vein. D. Dull to moderately orange luminescent calcite PC2 with non-luminescent dolomite (PD1) with bright red luminescent cracks (see arrows) cut by a vaguely zoned orange calcite PC3. E. Dull luminescent PC2 with cleavage twins, cross-cut by a zoned orange calcite PC4 vein, displaying a wispy luminescence texture. (For interpretation of the references to color in this figure legend, the reader is referred to the web version of this article.)

It is followed by a more brightly zoned orange calcite (PC4)(Fig. 3B, E), which displays the same CL-colour as spots in the neomorphosed matrix. Macroscopically these open veins are beige coloured and non-ferroan. Here cleavage twins are absent (Fig. 3E). The last open vein cement phase consists of some broadly zoned dull brown luminescent calcite (PC5), also without cleavage twins. There exists locally a corrosive contact between the brightly zoned (PC3) and the dull brown luminescent (PC5) calcite (Fig. 4A). Macroscopically these veins have a white non-ferroan nature. In some veins, a non-luminescent dolomite phase (PD1)(Fig. 3E), characterised by small red luminescent cross-cutting

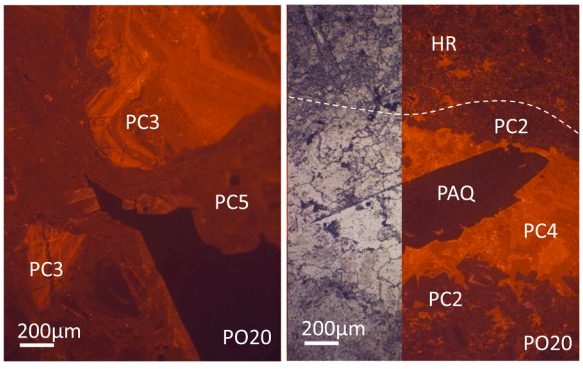

Fig. 4. Representative illustrations of diagenetic features in the Poederlee borehole samples (coloured parts are taken under cathodoluminescence while grey parts are taken under transmitted light microscopy). A. Corrosive contact between zoned orange calcite PC3 and dull luminescent PC5. B. Recrystallised host rock (HR) bordered by dull brown luminescent PC2. The central part of the vein is filled by zoned orange calcite PC4, in which a transparent authigenic quartz crystal (PAQ) is floating. (For interpretation of the references to color in this figure legend, the reader is referred to the web version of this article.)

fringes, developed that are crosscut by the zoned orange luminescent calcite veins (PC3)(Fig. 3D). Transparent authigenic quartz (PAQ) in veins (Fig. 4B) seems to cluster near these dolomite phases, and locally floats in the brightly zoned calcite (PC4).

Based on the observations described above, the diagenetic succession is interpreted as follows: firstly, fenestrae and open cavities in the cryptalgal limestones became cemented by fibrous and radiaxial marine cements but were subsequently neomorphosed and overgrown by meteoric zoned cements (Muchez et al., 1991b). With regard to the veining history it is obvious that many veins were reactivated. The most interesting observation, however, is that the first major vein generation PC2 displays well-developed cleavage twins while the subsequent vein generations do not or do sporadically display this feature. PC2 thus testifies from some tectonic stresses after their formation. The fluctuations in overall luminescence colour reflect differences in calcite chemistry and thus changes in the water chemistry or crystal growth (ten Have and Heijnen, 1985). However, overall the CL colours are rather uniform supporting cementation in the burial realm (Muchez et al., 1991b). The corrosive contact between vein generations reflect some important changes in fluid chemistry. The fact that transparent authigenic quartz phases occur in PC4, indicates that some silica was mobilised after this calcite cementation.

Most of the lithologies studied in the Heibaart borehole consist of mudstone and peloidal wackestone. They are either non- to dull luminescent but in some cases they clearly are affected by recrystallization as reflected by their blotchy yellow orange luminescence. In some cases the micrite even displays a bright orange luminescence. Typical for many lithologies is the presence of euhedral bipyramidal zoned and elongated authigenic quartz crystals, which can be up to 2 cm in length. They locally form clusters or are grouped along bed parallel stylolites. The zoned nature is caused by calcite impurities that often mark the core of the crystals but that also may occur in growth zones. The impure areas in the quartz crystals display a blotchy yellow orange luminescence while the more pure quartz phases are non-luminescent. In some of the cryptalgal host lithologies original pores are filled first by blotchy orange luminescent impure skalenohedral crystals upon which a dull zone follows before the more transparent central part with faint sector zoned orange luminescent blocky calcites follows (Fig. 5A). Within the latter some cleavage twins can be differentiated. At other places the first cement generation consists of non-luminescent equidimensional calcite rims (Fig. 5B, HC2), followed by a brown luminescent calcite similar to vein infilling phases (subsequently called HC3). Notice that the latter also contains some cleavage twins (Fig. 5B). Where crinoids acted as a substrate, zoned dogtooth cements locally developed starting with some dull luminescent zones followed by highly zoned overgrowths (Fig. 5C). In samples HE20 & 22 the matrix has been partially dolomitised as manifested by the red luminescence. Only in the latter lithologies some (intracrystalline) matrix porosity (<5%) occurs.

With regard to the veins in the Heibaart samples, several types can be differentiated, however, their mutual relationships are often not clear due to the absence of systematic cross-cutting relationships. Thus the numbering is not necessarily related to the paragenetic sequence, however, in some cases they reflect subsequent stages. In sample HE20 some red luminescent blocky dolomite (HD1) is present in a few veins, which sometimes displays saddle-like outlines and undulous extinction under crossed polarizers. This dolomite is followed by a uniformly orange luminescent blocky calcite (HC1) upon which a blotchy bright yellow calcite (HC2) precipitated that often fills up the remaining porosity. Both veins are macroscopically white coloured and slightly ferroan. Furthermore the blotchy luminescence of the latter calcite clearly reflects some recrystallization. In other samples a dull brown blocky calcite occurs (HC3) as the first infill (Fig. 5D & E) in macroscopically white veins that are non- to slightly ferroan. These completely cemented veinlets are reactivated, i.e. re-opened, and partially to completely filled by bright orange luminescent medium-sized (80-130 µm) calcite (HC4) (Fig. 5D). The latter crystals are sometimes faintly to

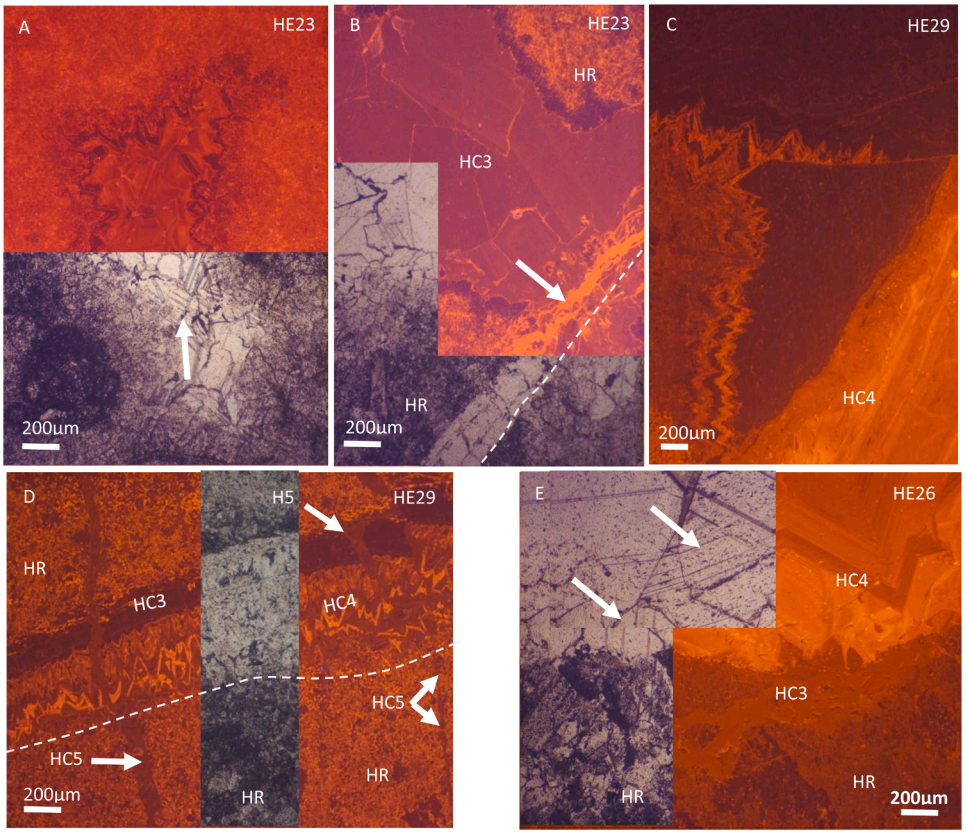

Fig. 5. Representative illustrations of diagenetic features in the Heibaart samples (coloured parts are taken under cathodoluminescence while grey parts are taken under transmitted light microscopy). A. Original cavity in cryptalgal limestone filled by inclusion-rich skalenohedral CL zoned calcite which becomes more transparent and coarse crystalline towards the centre. Some faint fibrous calcite cement can be recognised near the border of the pore. Notice also the presence of cleavage twins (see arrow) in the transparent calcite. B. Recrystallised host rock (HR) bordered by a non-luminescent calcite rim, before the remaining cavity is filled by dull brown blocky calcite (HC3), that subsequently was crosscut a yellow bright irregular calcite veinlet (see arrow; HC4). C. Crinoid fragments overgrown by CL-zoned dogtooth cements, engulfed in a bright orange luminescent calcite (HC4). D. Recrystallised host rock (HR) displaying some blotchy luminescence, crosscut by a brown luminescing calcite vein (HC3) that was reactivated before being filled by a zoned calcite with some bright zones (HC4). The latter is on its turn crosscut by a brown luminescent calcite (HC5)(see arrows). E. Partially recrystallised host rock (HR) crosscut by a brown luminescing calcite (HC3) and a zoned bright luminescing calcite (HC4) with faint cleavage twins (see arrow). (For interpretation of the references to color in this figure legend, the reader is referred to the web version of this article.)

clearly zoned. In Fig. 5D it is clear that the latter two white coloured veins which are aligned, are crosscut by another brown luminescent calcite generation (HC5). The latter is white coloured and non- to slightly ferroan. The complexity of vein filling phases can also be seen in Fig. 6A. Here HC3 is reactivated and subsequently refilled by HC4, which is in contact with a non- to dull luminescent blocky vein infill (HC6) displaying on its turn an irregular contact with an orange luminescent blocky calcite (HC7) possessing some brown luminescent irregular spots. The latter calcite is sometimes zoned. The latter four veins cannot be differentiated macroscopically since they all possess a white colour. The veins HC3 till 7 are partially open. In sample HE25 & HE26, however, it is clear that a dull blocky calcite vein generation (HC3), pre-dates a zoned orange luminescent calcite vein infill (HC4) while in sample HE24 this is the reverse, confirming the existence of two brown luminescing cement generations, as is also visible in Fig. 5D. Overall the dull blocky vein generation (HC3 or 5) and the orange blocky luminescent calcite (HC4) are the dominant cement phases in the open veins. Notice that the latter calcite generations display sometimes some

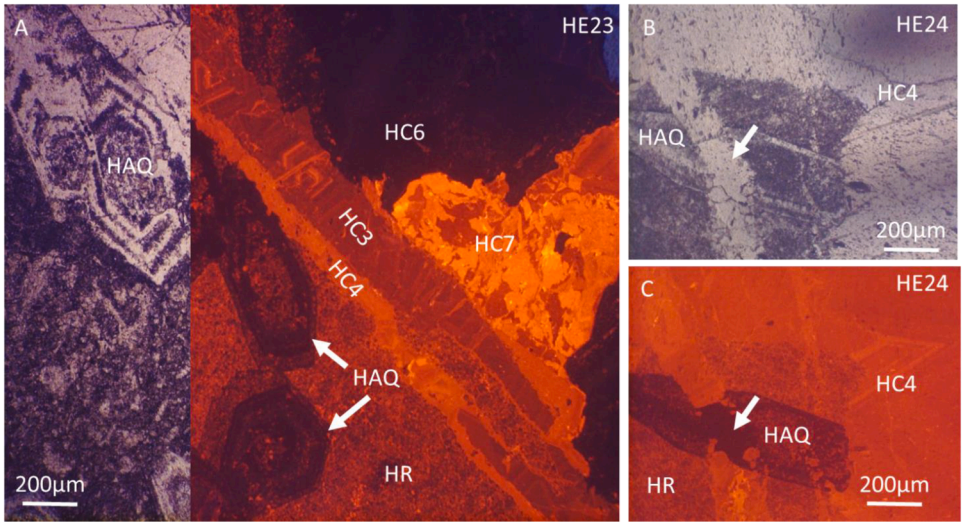

Fig. 6. Representative illustrations of diagenetic features in the Heibaart borehole samples (coloured parts are taken under cathodoluminescence while grey parts are taken under transmitted light microscopy). A. Blocky dull luminescent calcite (HC3) is reactivated and subsequently filled by a bright orange luminescent calcite (HC4), which is in contact with a non- to dull luminescent blocky vein cement (HC6) also containing an orange luminescent blocky calcite (HC7) possessing some brown luminescent irregular spots. The contact between HC6 and 7 is irregular. The host rock (HR) displays a non-uniform luminescence testifying of recrystallization. Within the latter some zoned authigenic quartz (HAQ) crystals occur. B. & C. Respectively transmitted and cathodoluminescence photomicrograph of same area. Recrystallised host rock (HR) bordered by bright orange luminescent calcite (HC4). Within the host rock an authigenic crystal (HAQ), rich in impurities, occurs. Notice that where the authigenic quartz is crossed by the calcite vein some transparent syntaxial quartz developed (see arrow). (For interpretation of the references to color in this figure legend, the reader is referred to the web version of this article.)

faint crystal cleavage twinning. In addition, a noteworthy feature with regard to the authigenic quartz crystals is that where they are cut by a vein, locally some transparent overgrowth quartz developed within the veins (Fig. 6B).

The earliest matrix porosity infill phases in the Heibaart borehole, such as the impure relict fibrous crystals in the impure skalenohedral crystals or the first dull luminescent dog tooth overgrowth on crinoids most likely have a marine phreatic origin (Muchez et al., 1991b). The subsequent zoned overgrowth cements likely developed in a meteoric phreatic realm. The authigenic quartz phases in the matrix developed after compactional stylolites formed. Based on their zonation pattern, some fluctuations in quartz saturation occurred during their growth. Nearly all limestones testify of some neomorphism. The veining history clearly is complex, with sometimes uniformly luminescent calcite infills pointing towards geochemical uniform and thus burial conditions. The sometimes CL-zoned cement phases indicate some variation in the crystallisation conditions. Reactivation and thus opening of former calcite veins has been regularly observed. Several of the blocky vein cements (HC3 and HC4) possess cleavage twins. Therefore, they likely formed before some tectonic deformation. Vein infill HC5 to 7 do sometimes display cleavage twins. Where authigenic quartz crystals are cut by a vein, the small transparent overgrowth on the quartz crystals testifies of a minor flux of a Si-rich fluid after vein formation.

The studied limestones from the Turnhout borehole display clear indications of recrystallization, indicated by the existence of dull and yellow bright luminescent microspar. Larger crystals contain frequently small impurities of former fine crystalline calcite phases. In some lithologies, birdseye type pores are filled by non-bright-dull (NBD) zoned calcite cements (Fig. 7A). Locally the zonations are blurred due to recrystallization.

Different vein generations have been recognized, which are filled by blocky uniform yellow to orange (sometimes faintly zoned) luminescent calcite (TC1, Fig. 7C)(macroscopically displaying a non-ferroan white colour) or uniform brown luminescent calcite (TC2; Fig. 7B) (macroscopically displaying a non-ferroan white or grey-white colour). Based on the isotope results presented below it will become clear that most likely two uniform brown luminescent calcite (TC2A & B) exist, that affected the limestones at different depth positions. Most former calcite veins show clear cleavage twinning. Notice that since the paragenetic succession is also unclear in this borehole, the numbering not necessarily reflects the paragenetic succession. Some of the veins are bordered by stylolites (Fig. 7B). In some stylolites, bordeaux red luminescent dolomite phases (TD1) (macroscopically displaying a rose colour and being non-ferroan) occur as well as some bitumen. In some samples, larger bright bordeaux red zoned dolomite rhombs (TD2)(also rose in colour macroscopically), sometimes with saddle outline and an undulose extinction under polarizing light, occur (Fig. 7C). The dolomite rhombs formed after the yellow orange bright calcite TC1 which sometimes are partly engulfed by the dolomites. All veins (TC1 & 2 and TD1 & 2) can form (partially) open veins. In sample TU22 some very thin parallel-oriented veinlets filled with a non- to dull brown luminescent calcite phase (TC3; Fig. 7C) occur as the latest phase next to quartz infill. The crystals within these veinlets develop perpendicular to the vein walls forming a kind of bridges. Some of these veinlets possess some porosity between the crystals.

The NBD matrix cements could have both a marine (Savard and Bourque, 1989) or meteoric phreatic origin (Walkden and Berry, 1984). The TC2 veins bordered by stylolites seem to predate pressure dissolution. Most of them also suffered from tectonic deformation as attested by the cleavage twins present. Most vein cements display a rather uniform luminescence suggesting burial conditions during their formation. The (saddle) dolomite post-dates the blocky (TC1) calcite infill, however, it is crosscut by very thin, parallel-oriented dull luminescent calcite (TC3) and quartz-bearing veinlets. The latter are marked by a crystal growth perpendicular to the walls, supporting simultaneous growth while the veinlets were opening.

4.3. Stable isotope geochemistry

The stable isotope data (Supplementary data Table 1) from the Poederlee borehole (Fig. 8A) and the Heibaart borehole (Fig. 8B) clearly overlap. The data plot between -8.77‰ and -14.27‰ for $\delta^{18}O_{PDB}$ and between +2.78‰ to -2.89‰ for $\delta^{13}C$. However, with the exception of one value, the cluster from Poederlee (Fig. 8A) is somewhat smaller with less samples with depleted $\delta^{13}C$ values. The stable isotope data of host rock and calcite cement phases from veins from the Turnhout borehole (Fig. 8C), with the exception of 3 samples with a negative $\delta^{13}C$ varying around -2‰, display a faint positive correlation between $\delta^{18}O_{PDB}$ and $\delta^{13}C$ values, respectively varying between -17.88‰ to -6.83‰ and between +0.83‰ and +3.44‰.

More in detail, the host rock and the calcite vein cements from the same samples from the Poederlee borehole possess rather similar stable isotope values, e.g. samples PO 15, 20 (with exception of sample PO20.2) and 23 (Fig. 8A). However, in most samples there is a moderate spread in $\delta^{13}C$ as well as in $\delta^{18}O_{PDB}$ but the maximum spread is not larger then about 4‰. Noteworthy is that the isotopic signatures of PC2 to 5 do not display any systematic difference.

In the Heibaart samples (Fig. 8B) two clusters of stable isotope data can be differentiated, i.e. a cluster where the host rock displays nearly the same stable isotope signature as the veins (e.g. samples HE22, 27 and 28 with HC2 and HC3 veins), and samples where the host rock is more positive with regard to both the carbon and oxygen isotope data than the

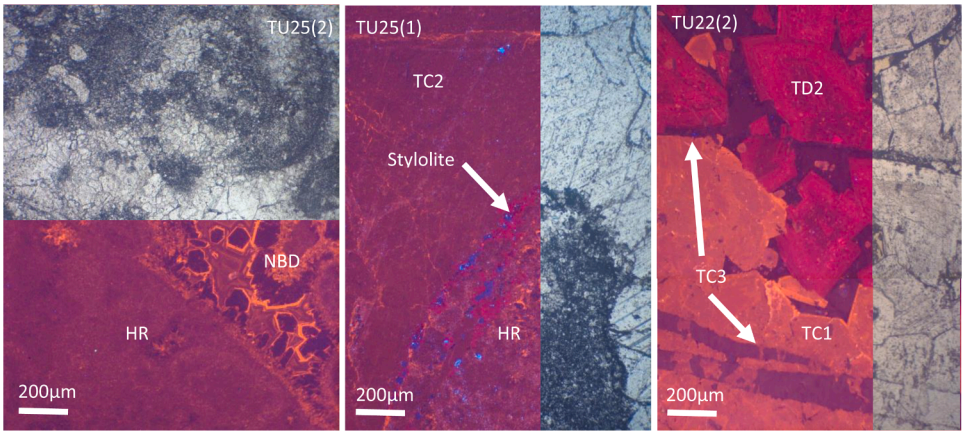

Fig. 7. Representative illustrations of diagenetic features in the Turnhout samples (coloured parts are taken under cathodoluminescence while grey parts are taken under transmitted light microscopy). A. Recrystallised host rock (HR) with primary cavity filled by non-bright-dull (NBD) zoned calcite cements. B. Contact between recrystallised host rock (HR) and uniform brown luminescent calcite (TC2). At their contact a burial stylolite developed. The blue spots in the host rock and stylolite correspond to polishing powder that remained in some of the pores. C. Contact between yellow orange bright calcites (TC1) and bright bordeaux zoned dolomite rhombs (TD2), both crosscut by non- to dull brown luminescent calcite veinlets (TC3). (For interpretation of the references to color in this figure legend, the reader is referred to the web version of this article.)

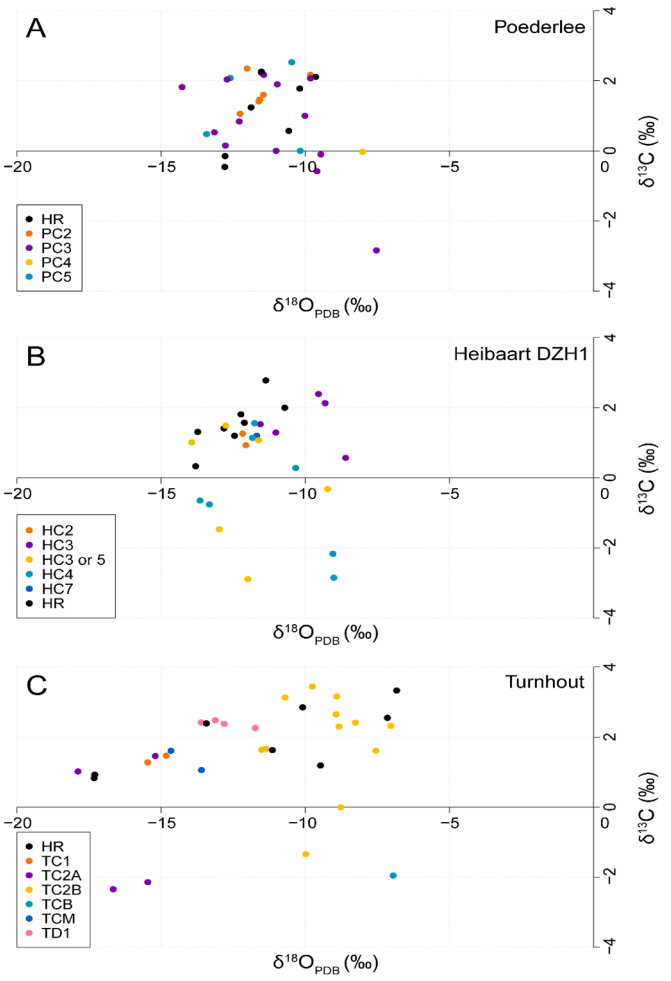

Fig. 8. Stable C- and O-isotope cross plot of Poederlee samples (A), Heibaart samples (B) and Turnhout samples (C) classified according vein types (HR = host rock). Information on vein types see Section 4.2.

veins, especially with regard to their $\delta^{13}C$ signature (with up to 4.85‰ V-PDB difference) while their $\delta^{18}O_{PDB}$ values differ only by maximum 2.2‰. In the latter group HC3, HC4 and HC5 veins occur. Notice that HD1 neither HC6 have been analyzed for stable isotopes since these phases were too small to be sampled individually.

The stable isotope data of the Turnhout samples (Fig. 8C) cluster rather well together (host rock and veins), with the exception of sample TU24, where the veins are much more depleted in carbon and oxygen stable isotopes, as well as for sample TU23 where the sampled brachiopod displays curiously enough a negative $\delta^{13}C$ signature of -1.95‰ and a negative $\delta^{18}O_{PDB}$ value of -6.95‰. In the same sample, the cement infill in fenestrae-like pores, of which one phase clearly displays characteristics of marine cementation, possess very depleted $\delta^{18}O_{PDB}$ values as low as -14.66‰ and -13.60‰. Within the uniform brown luminescing veins, two clusters can be differentiated based on the $\delta^{18}O_{PDB}$ values, i.e. one cluster (TU2A) with very depleted values dominantly plotting between -18‰ to -15‰ and a second cluster (TU2B) with values plotting dominantly between -11‰ to -7‰.

As a general observation, one can state that the $\delta^{18}O_{PDB}$ isotopic signatures of most host rocks have been reset due to the interaction with meteoric fluids or with fluids at higher temperature (cf. Muchez et al., 1991a, b; 1994a). With regard to the $\delta^{13}C$ signature of the host rocks, the latter is often similar to that of marine carbonates. However, in certain cases, the low carbon isotopic composition indicates that a partial contribution of a depleted carbon source needs to be invoked. Since most of these veins can be classified as burial in origin, a most likely source for the latter is the contribution of organic material. However, this C-source clearly mixed with the host rock derived carbon source, which remained the dominant source (cf. Muchez et al., 1994a).

4.4. Clumped isotope geochemistry and inferred carbonate precipitation temperatures

In total 12 cement phases have been analyzed. In three cases, 2 samples were taken from the same open vein. This was possible where individual cement phases could be differentiated or where the vein cement was wide enough to take a sample near the vein wall and from the center. The inferred temperatures vary between 48 and 216 °C. Roughly a grouping can be seen between 48 to 66 °C, 78 to 89 °C and 109 to 129 °C, with one outlier of 216 °C. Notice also that the highest standard deviation relates to the analyzed saddle dolomites (sample TU20 vein type TD1).

Since apart from the inferred formation temperature based on the clumped Δ_{47} isotope also the $\delta^{18}O_{PDB}$ of the carbonates was analyzed, it is possible to calculate the isotopic composition of the ambient fluid based on the equation of O'Neil et al. (1969) for calcite-water fractionation and the equation of Land (1983) for dolomite fractionation.

In the Poederlee borehole two samples of dull brown luminescent non-ferroan calcite (PC2) with cleavage twins gave an inferred temperature of 122 ± 6 °C and 129 ± 4 °C (respectively for samples PO15C and PO15I), which results in water oxygen isotope signatures of +4.7 ± 0.7‰ and +6.3 ± 0.3‰ $\delta^{18}O_{SMOW}$, respectively. Sample PO20 consisting of yellow brown luminescence PC4 (non-ferroan) calcite gave a temperature of 66 ± 4 °C and a calculated $\delta^{18}O_{SMOW}$ value of +1.4 ± 0.8‰.

The most interesting sample in the Heibaart borehole is sample HE24, where the oldest calcite generation HC4 has a temperature of 124 °C while the younger cross-cutting vein cement HC7 (HE24O) yields a temperature of 51 °C. The highest temperature sample yields a $\delta^{18}O_{SMOW}$ signature of +3.9 ± 0.3‰, while the younger vein generation results in a $\delta^{18}O_{SMOW}$ signature of -4.9 ± 0.7‰. The other samples, i.e. HE22, HE28 and HE25 have a precipitation temperature of 48 ± 6 °C, 62 ± 3 °C and 89 ± 5 °C, respectively. These temperatures resulted in respective $\delta^{18}O_{SMOW}$ values of -5.3 ± 1.0‰, +0.2 ± 0.3‰ and +1.2 ± 0.5‰.

Four samples were analyzed from the Turnhout borehole of which TU20 consists of 2 generations of TD1 dolomite (with the oldest generation containing pyrite inclusions). They yielded a temperature of respectively 78 ± 8 °C and 80 ± 9 °C, resulting in a $\delta^{18}O_{SMOW}$ value of -5.2 ± 1.0‰ and -5.5 ± 1.1‰ respectively. Cement TC1 of sample TU23 with an orange luminescence yields a temperature of 109 ± 4 °C, resulting in a $\delta^{18}O_{SMOW}$ of +0.5 ± 0.4‰ while the red brown luminescent non-ferroan calcite T2B of sample TU25 with cleavage twins has the highest calculated temperature of 216 ± 6 °C, resulting in a $\delta^{18}O_{SMOW}$ signature larger than +17‰.

A general decrease of the oxygen isotopic composition of the ambient fluid with lower precipitation temperature is observed. In a rock-buffered oxygen isotopic system, this is indeed a normal consequence (Warr et al., 2021). The lowering of the oxygen isotopic composition of the fluid is therefore not necessarily due to a mixing or replacement of the pore fluid with a fluid with a lower oxygen isotopic composition but can be just due to the lowering of the temperature in a rock-buffered system. However, it cannot exclude that fluids with a lower oxygen isotopic composition such as meteoric or sea water did infiltrate the subsurface.

4.5. U/Pb dating

In total 8 samples were selected for U/Pb dating. Unfortunately only 3 reliable age dates were acquired (see Figs. 9 to 12). The unsatisfactory U/Pb dating results can have several reasons, such as too low U/Pb variability or too high initial Pb. Another possibility relates to recrystallization with no uniform resetting (Fig. 9)(see also Godeau, 2018).

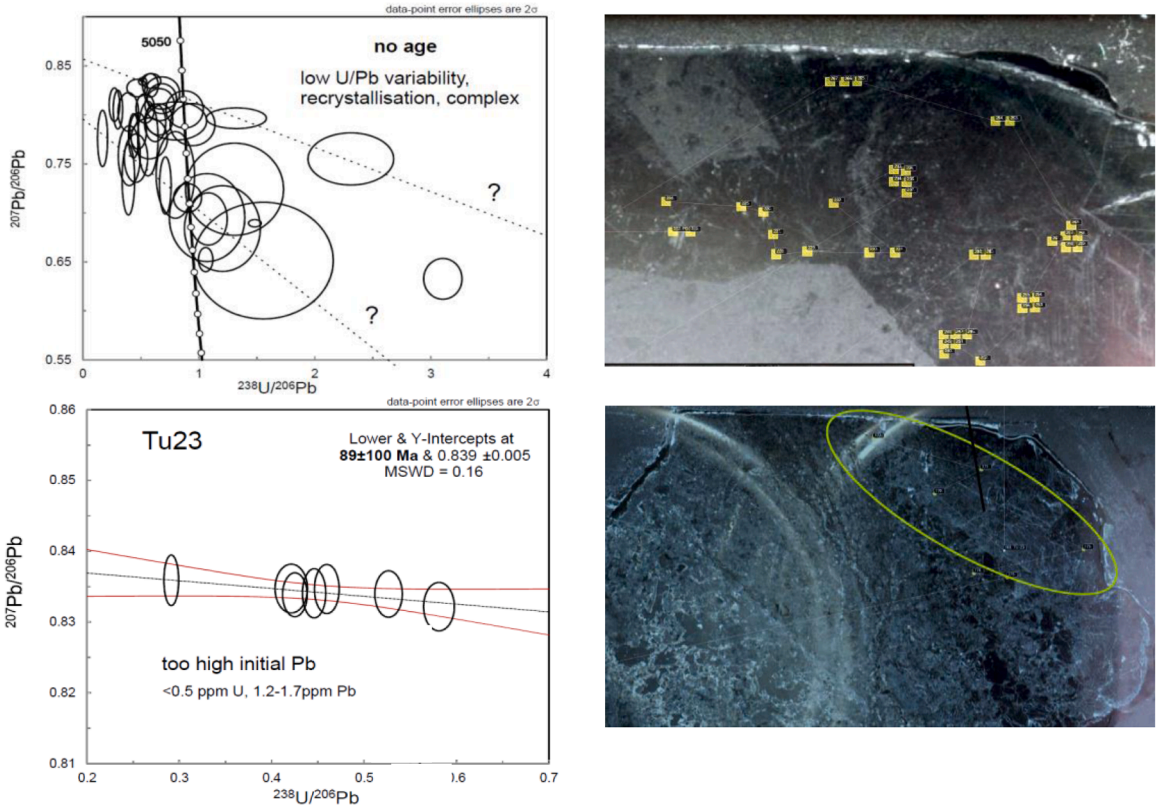

Fig. 9. Tera Wasserburg plots of vein PO17 (upper picture; vein type PC3) and TU23 (lower picture; vein type TC1) with indication of clusters from where the data were retrieved. Based on the clustering of the data no reliable age dating was possible.

However, the three ages acquired are relevant.

The most trustworthy age dating is from sample PO20 (Fig. 10; vein type PC4), where 3 clusters were sampled in the same calcite vein, giving a rather consistent age varying between 113.2 ± 0.7 Ma and 110.1 ± 3.7 Ma. Sample HE22 (Fig. 11; HC7) yields an age of 113.0 ± 2.6 Ma. In sample TU20 two dates were acquired for the TD1 dolomites,

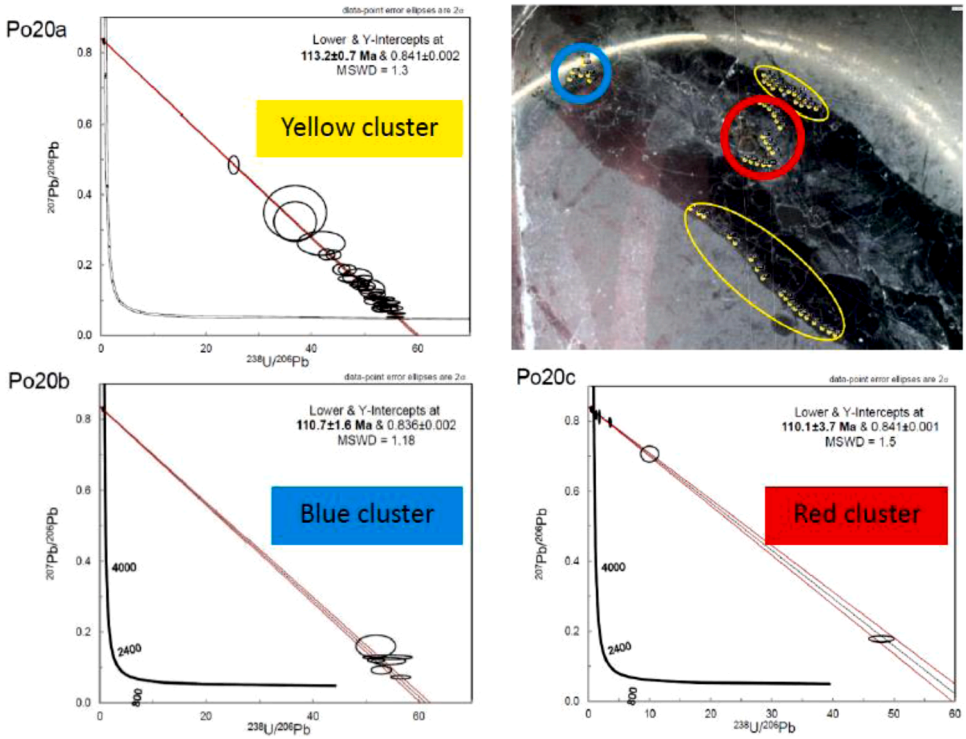

Fig. 10. Tera Wasserburg plots of vein PO20 (vein type PC4) with indication of clusters from where the data were retrieved.

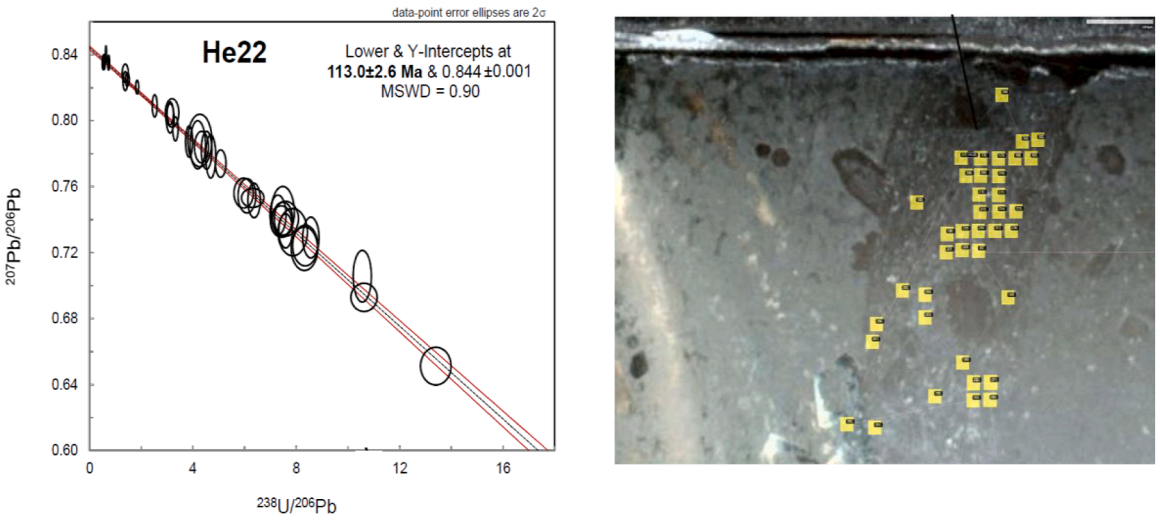

Fig. 11. Tera Wasserburg plots of vein HE22 (vein type HC7) with indication of clusters from where the data were retrieved.

despite that both display the same crystallization temperature (based on clumped isotopes). One cluster, that correspond with only three sampling points taken from the oldest part of the vein near its border with the host rock (Fig. 12) yields an age of 27.4 ± 3.1 Ma, while the much larger cluster with sampling points all over the vein including positions from its more central younger part gives an age of 59.3 ± 1.2 Ma. The latter age seems the most trustworthy based on the larger consistent dataset used. Thus based on this limited dataset, vein development took place near the Aptian and Albian boundary and during the Mid-Paleocene.

4.6. *Burial history*

To be able to place the formation of the open veins into the burial history of the boreholes in the Campine Basin, published data were consulted from Van Keer et al. (1998), Helsen and Langenaeker (1999) and Bertier et al. (2008). These authors relied their reconstructions on vitrinite reflectance data that mainly originated from the overlying coal-bearing Westphalian sandstones and organic-rich Namurian shales. Our reconstruction of the burial history of the Poederlee and Turnhout boreholes (Fig. 13), which are also representative for the Heibaart borehole, is in line with the first and last cited authors, where more detailed information based on which criteria the burial history was reconstructed can be consulted. Here we give only some key information

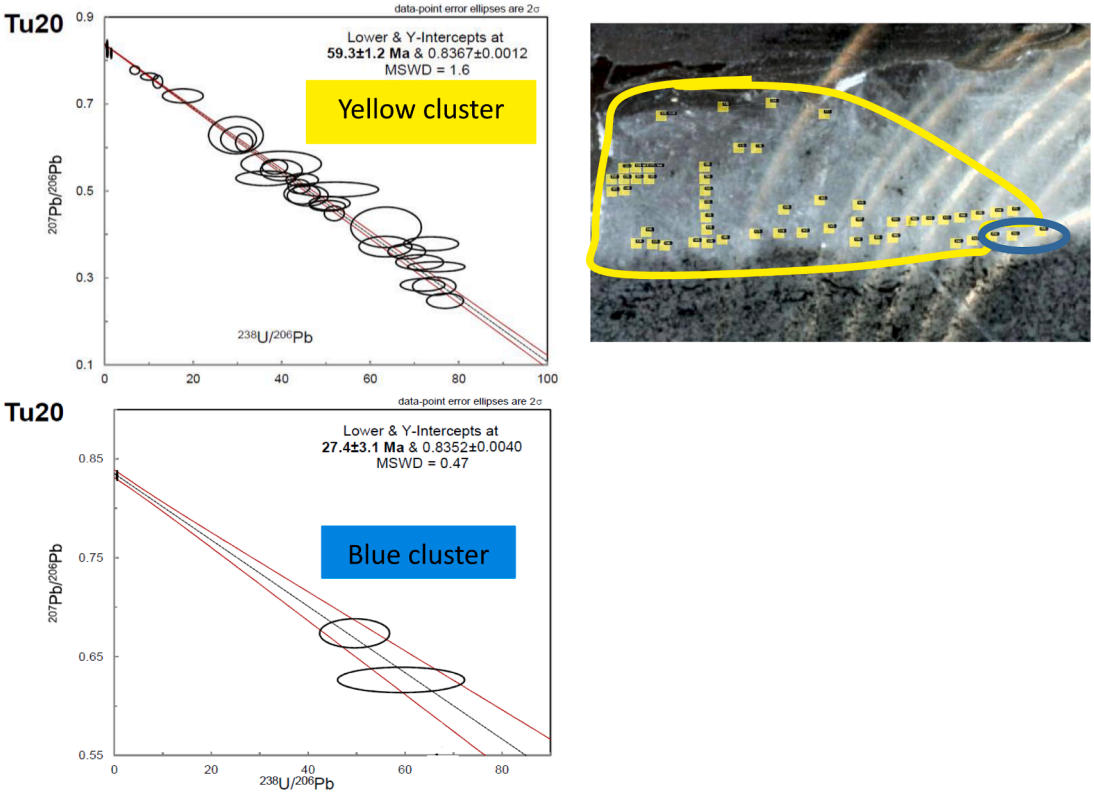

Fig. 12. Tera Wasserburg plots of vein TU20 (vein type TD1) with indication of clusters from where the data were retrieved.

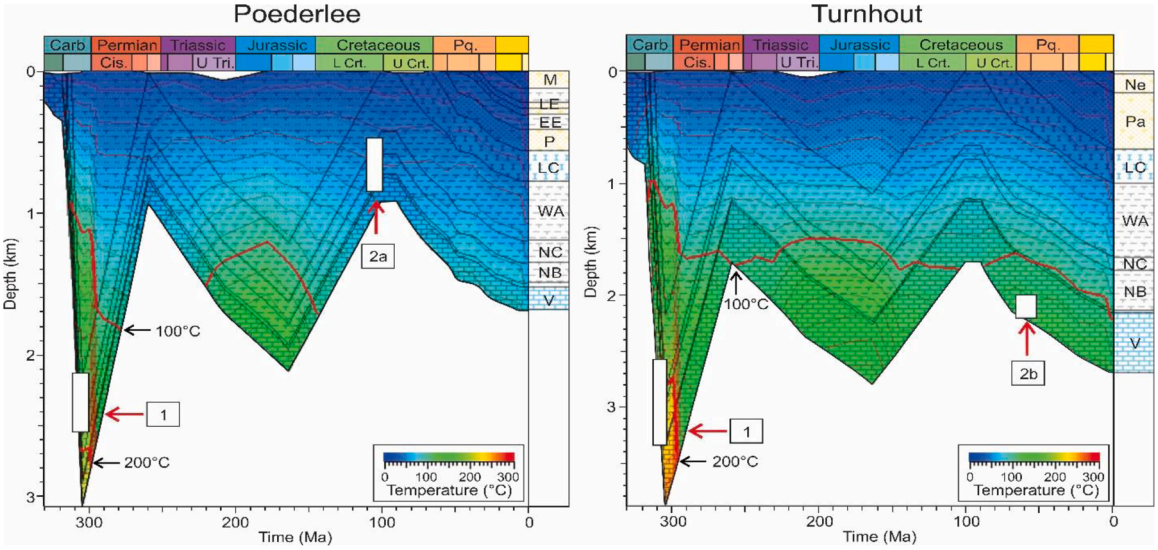

Fig. 13. Burial history and temperature evolution starting at the top Dinantian in the Poederlee (left) and Turnhout (right) borehole with indication of at least 2 fracturing events (1 and 2a & 2b). Note that the thickness of the Dinantian strata need to be added to assess the real maximum burial and temperature. Abbreviations: V: Viséan; NB: Namurian B; NC: Namurian A; WA: Westphalian A; LC: Late Cretaceous; P: Paleocene; EE: Early Eocene; LE: Late Eocene; M: Miocene; Pa: Paleogene; Ne: Neogene.

needed for the discussion session.

During the Lower Carboniferous marine limestones accumulated in the block faulted Campine Basin. At the end of the Viséan a major regression affected the area related to the Sudetic tectonic phase, which was followed by the deposition of open marine (organic-rich) Namurian shales and subsequent thick Westphalian coal measures deposited in the Variscan foreland setting. The different diagenetic modifications of the Dinantian limestones with several stages of vein development reported by Muchez et al. (1991a) relate to this first burial cycle. As can be seen in Fig. 13, temperatures reached approximately 200 °C and 230 °C in Poederlee and even higher in Turnhout, respectively. During the Late Carboniferous and Early Permian the basin was uplifted in relation to the northward prograding Variscan orogeny with partial erosion of Upper Westphalian sediments. In the north-east of the Campine Basin, the Westphalian strata became covered by thin Zechstein conglomerates and carbonates, before Mesozoic strata started to accumulate. The latter mainly consist of thick Buntsandstein sandstones. During the Jurassic the basin underwent the Cimmerian tectonic phase with first extensional tectonics that caused the main subsidence in the Roer Valley Graben, in which Jurassic deposits were preserved. It is, however, unclear how much Jurassic sediments accumulated and subsequently were eroded in the western Campine Basin, therefore the burial curves and related temperatures shown in Fig. 13 are tentative. Unfortunately no fission track data are available from the study area. But it is rather unlikely that very thick sediments accumulated since the sedimentary wedge is pinching out towards the Brabant Massif. The extensional regime was followed by two compressive tectonic events, the first occurring at the end of the Jurassic and the second at the beginning of the Late Cretaceous (Rossa, 1986). This led to the end of the second burial cycle. As a result the entire basin was tilted, explaining the angular unconformity between the older strata and the overlying Cretaceous deposits. The latter cover the entire succession from Devonian strata in the south and Jurassic (and locally Zechstein) sediments in the north. The thickness and facies distribution of the Cretaceous strata relate to the inversion tectonics of the Alpine Orogeny. The created fault system became subsequently reactivated during the Paleocene (Laramide phase, Alpine). The peneplain of the Laramide phase is covered by mainly clastic Cenozoic strata, reaching locally thicknesses of several hundreds of metres.

5. Discussion

With regard to the paragenesis of the Dinantian carbonates (host rock diagenesis and fully cemented veins in the Campine boreholes) we refer to Muchez et al. (1991a, b). As mentioned above, the focus of this study is on the open veins. With regard to the inferred burial depths mentioned below they were derived by accepting a thermal gradient of 30 °C/km with a surface temperature of 20 °C, and assuming equilibrium precipitation between fluids and host rock (thus not taking hydrothermal fluids into account, however, this aspect will also be addressed). To be able to place the vein development in its geodynamic evolution, the burial and temperature evolution for Poederlee and Turnhout borehole will be used as given in Fig. 13. Unfortunately no fluid inclusion data are available that could independently assess the temperatures deduced from clumped isotopes.

The range in the oxygen isotopic composition of the Upper Viséan host rocks is much lower than the values of Lower Carboniferous marine carbonates ($\delta^{18}O_{PDB}$ by +1.5 ± 2‰ and $\delta^{13}C$ value of +2.6 ± 2‰; Brand, 2006). These lower oxygen isotope values can be explained by recrystallization of the limestones by meteoric water which infiltrated the subsurface at the end of the Viséan (Muchez et al., 1991b), however, recrystallization by interaction with other fluids during the first burial cycle cannot be excluded. The carbon isotopic composition of the limestones studied largely plot within the range of Lower Carboniferous marine carbonates and indicates buffering of the carbon isotopic composition by the limestones. Some of the slightly lower carbon isotope values of the limestones (Fig. 8) can also be explained by the influx of the meteoric water with low carbon isotope values originating for example from organic soil material (Muchez et al., 1993). This, however, also possibly relates to the maturation of organic material present in the Upper Carboniferous shales located around the mound structures at Poederlee and Heibaart but also being intercalated in the uppermost part of the Lower Carboniferous and occurring abundantly in the lower part of the Upper Carboniferous. Thus the recrystallization of the host rocks might also relate to interaction with these fluids.

The range of oxygen and carbon isotopic values of the different vein cements analyzed broadly overlaps with the stable isotopic composition of the host rock. In the different boreholes the number of veins with negative carbon isotopic values is larger than the number of host rocks and values can be as low as -3 ‰ V-PDB. This can be explained by the

mixing of carbon derived from the limestones with carbon derived from the maturation of organic material (Irwin et al., 1977).

More specifically the samples with the highest precipitation temperatures in the Poederlee borehole (122 ± 6 °C and 129 ± 4 °C) taken in the dull brown luminescent sometimes broadly zoned non-ferroan PC2 calcites possess $\delta^{18}O_{SMOW}$ signatures of +4.7 ± 0.7‰ and +6.3 ± 0.3‰, respectively. They could be related to evolved residual brines that were already present in the subsurface since the late Carboniferous. Such evolved fluids indeed were identified by Muchez et al. (1991a) in his study of vein types that formed before and during maximum burial in the Campine Basin. The calcite cement without cleavage twins at Poederlee and showing a yellow brown luminescence (vein type PC4) precipitated at a temperature of 66 ± 4 °C, formed after uplift and deformation during the Cretaceous, as attested by its late Aptian/early Albian age. The inferred $\delta^{18}O_{SMOW}$ value of +1.4 ± 0.8‰ is lower than the previously mentioned values. This lower calculated oxygen isotopic value could be due to the lowering of the precipitation temperature in a rock-buffered system or could reflect a mixture of the evolved fluid with a high oxygen isotopic signature with a fluid with a much lower oxygen isotopic composition (e.g. meteoric signature) or replacement of the basinal fluid by a seawater-dominated fluid. The calculated precipitation depth of the vein cementation is 1.5 km which is more than the current thickness of the Namurian and Westphalian sedimentary pile below the Late Santonian (Upper Cretaceous; Vandenberghe et al., 2004). This could indicate that about 700 m of Westphalian strata have been eroded after this cement formed and before deposition of the Cretaceous in this part of the basin.

The high temperature calcites in Poederlee possibly formed during the first burial cycle in relation to the Sudetic/Asturian deformation stage, an interpretation that is supported by the cleavage twins which characterise these vein generations. However, their formation during the uplift cycle or during the second burial cycle cannot be excluded since no conclusive datings could be acquired. The lower temperature veins of Upper Aptian/Lower Albian age likely relates to the switch from uplift to renewed burial in relation to the stress regime induced by the far field Alpine orogeny. This is in line with the complex subsidence and uplift history during the Upper Cretaceous in the Campine Basin as reported by Vandenberghe et al. (2014)

In Heibaart, sample HE24 is of special interest since here the oldest ferroan HC4 calcite vein with cleavage twins yields a temperature of 124 °C, while the younger cross-cutting non-ferroan HC7 sample without cleavage twins yields a temperature of only 51 °C. This results in calculated $\delta^{18}O_{SMOW}$ signatures of +3.9 ± 0.3‰ and -4.9 ± 0.7‰, respectively. The oldest vein possibly formed time equivalent with the above cited PC2 Poederlee veins and thus a similar origin is tentatively invoked. This vein development clearly happened after the first burial cycle and uplift of the limestones. Sample HE22 yields an age of 113.0 ± 2.6 Ma with a calculated crystallization temperature of 48 ± 6 °C. The other two samples, that could not be dated gave respective temperatures of 62 ± 3 °C and 89 ± 5 °C corresponding respectively with burial depths of 1.4 km and 2.3 km.

In the Turnhout borehole, the TD1 dolomite (with pyrite inclusions in the oldest dolomite generation)(sample TU20) yielded temperatures around 80 ± 9 °C. In contrast, the ferroan saddle dolomites from the Poederlee borehole, reported by Muchez et al. (1991b), formed as the latest phase of the first burial cycle at very high temperatures (200 °C) and from evolved basinal fluïda. Based on these differences it is very likely that both coarse crystalline dolomites relate to different fluid systems, as also reflected by the non-ferroan nature of the Turnhout dolomites. The most trustworthy U/Pb date of 59.3 ± 1.2 Ma of the TD1 dolomite points to a Middle Paleocene age, with a calculated burial depth of 2 km, under the assumption that these dolomites do not relate to hydrothermal fluid circulation. A burial depth of 2 km for the Middle Paleocene seems possible, however, the reconstructed depth according to the burial history (Fig. 13) is somewhat shallower, thus questioning whether hydrothermal fluids were involved. Different fluid flow scenarios can be invoked, as discussed before, but a host rock buffered fluid that interacted with the Lower Carboniferous dolomites seems the most likely. The sample with TC2B cements with the highest temperature of 216 ± 6 °C (TU25) reflects the involvement of a fluid with a calculated $\delta^{18}O_{SMOW}$ signature >+17‰. Of interest here is that the maximum vitrinite Rmax value present at the top of the Lower Carboniferous in the Turnhout borehole is 2.8%, which corresponds, taking into account a coalification period of 20 Ma, with a temperature of 225 °C. Therefore it is likely that this cement formed during the first burial cycle (cf. Muchez et al., 1991b). If this is indeed the case, then the involvement of hydrothermal fluids can be excluded. With regard to the TC2 uniform brown luminescent calcite veins two generations could be differentiated based on their stable isotope signature. Noteworthy is that they occur at different depth in the borehole (see supplementary data Table 1), which supports the existence of two periods of their development. Finally with regard to the Turnhout covariance between $\delta^{18}O_{PDB}$ and $\delta^{13}C$ values (Fig. 8C) this relationship likely reflects the slight carbon fractionation with temperature as reported by Emrich et al. (1970).

At what stage the veins which could not be dated formed remains speculative. However, since all these vein cements form part of the open veins in the Poederlee, Heibaart and Turnhout borehole and since the oldest age of these vein cements is around 113 Ma, we postulate that they formed after burial during the Carboniferous and maximum burial in the Jurassic and thus during uplift. Based on the acquired data it is not unlikely that there were two independent fracturing events, one around 110-113 Ma (Fig. 13: stage 2a) and the second around 59 Ma (Fig. 13: stage 2b).

Thus based on the absolute age dating some fracturing and cementation events relate to tectonic activity spanning the Upper Cretaceous till Paleocene. This is in line with research carried out in outcrops in southern Belgium, France and the UK. Based on palaeostress records in Cretaceous formations in the Mons Basin (Belgium; Vandycke and Bergerat, 1989; Vandycke et al., 1991) and confirmed from Boulonnais (France) and Kent areas (UK) (Vandycke and Bergerat, 1992; Bergerat and Vandycke, 1994) as well as the Isle of Wight (Wessex Basin, UK; Vandycke and Bergerat, 2001) and NW Europe (Vandycke, 2002) synsedimentary Meso-Cenozoic strike-slip and extensional tectonic events have been documented. More recently, Duperret et al. (2012) reported on three main Upper Cretaceous extensive events, characterised by normal faulting and jointing and two Cenozoic compressive and extensional events with strike-slip and normal faulting along the English Channel in Normandy (France) and Sussex (UK). They relate these events to the geodynamic reorganisation as a consequence of the convergence between Eurasia and Africa and the opening of the North Atlantic area. Thus the data reported in this paper show that also the Campine Basin north of the Brabant Massif was affected.

The acquired results indicate that the targeted Campine Basin deep buried Lower Carboniferous carbonates were affected by Cretaceous – Paleocene tectonic stresses. Thus the above mentioned results from Cretaceous carbonates could have some relevance for better assessing the open fracture network in the subsurface. The development of secondary porosity is considered the most important factor in determining the prospectivity of the Lower Carboniferous carbonate play (Wintershall Noordzee, 2006; TOTAL 2007; Böker et al., 2012) and its potential for geothermal energy. But apart from fracturing, it should be reiterated that (meteogene as well as hypogene) karstification has been identified as another important process that may improve the reservoir potential of carbonates, however, the latter was not studied in this contribution.

The integration of different state of the art analytical techniques with conventional ones allowed to better constrain the diagenetic evolution in these potential geothermal limestone reservoirs. Therefore this study can serve as a guideline for similar studies elsewhere. One should consider the tectonic stress field during the Cretaceous – Paleocene that affected the Campine Basin when exploring the open fracture network in the Lower Carboniferous carbonates. Also with regard to the study of reservoir analogues, attention should be given to the study of Cretaceous

– Paleocene related fracture networks.

One can question why the veins we studied are only partly cemented. This implies that the ions (Ca^{2+}, Mg^{2+}, HCO_3^-) needed to cement the veins were not available in sufficiently high amounts to fully fill the fractures. This means that a local source of ions due to e.g. pressure solution or an external source due to fluid migration and supply of ions were not available in sufficient amounts. This is in agreement with the observation that the partly cemented veins cross-cut all stylolites or other evidence for pressure dissolution. Thus this source is not very likely. The absence of large scale fluid migration is also not very likely based on the observation of the partly cemented veins.

To come back to the potential involvement of hydrothermal fluids earlier diagenetic studies on vein cements in the Campine Basin confirmed that hydrothermal fluids migrated from the deeper basin along a growth fault to the margin of the platform during the initial stages of burial (Muchez et al., 1994b). However there is no evidence for hydrothermal fluids migrating through fractures on the shelf at that burial stage. The trapping temperatures of the fluid inclusions in all vein cements at the borehole of Poederlee were lower than or just near the maximum burial temperatures deduced from vitrinite reflectance data (Muchez et al., 1991a). The acquired data of the present study also do not provide evidence for hydrothermal fluid circulation during the Cretaceous - Paleocene.

6. Conclusions

For the first time crystallization temperatures deduced from clumped isotopes were acquired from open calcite veins from Lower Carboniferous carbonates from the Campine Basin (Belgium). The vein cements were characterized by petrography (including cathodoluminescence) as well as stable C- and O isotope analysis. An effort was also made to date the vein cements by U/Pb dating, however, only a limited number of samples gave reliable results, but the acquired dates reveal new insights in the diagenetic evolution of the Campine Basin.

Relatively high crystallization temperatures were acquired from calcite veins with cleavage twins. Both ferroan and non-ferroan dominantly blocky calcites make up this population. A remarkable feature in the Heibaart and Poederlee boreholes, and less developed in the Turnhout borehole is that a group of cement phases and their host rocks do not differ much with regard to their $\delta^{18}O_{PDB}$ signature. However, with regard to their $\delta^{13}C$ signature a shift in the order of 4 to 5‰ may occur, whereby the host rocks were least depleted and reflect a marine $\delta^{13}C$ signature despite that their $\delta^{18}O_{PDB}$ signature supports recrystallization by meteoric water and/or recrystallization by interaction with hot fluids. With regard to the veins studied, the higher temperature systems reached temperatures of 120-125 °C. They display enriched $\delta^{18}O_{SMOW}$ signatures which can be explained by buffering of the oxygen isotopic composition of the fluid by the host-rock at this temperature. The depleted $\delta^{13}C$ signature of these veins point to the fact that the resilient fluïda contained depleted CO_2 likely in relation to the maturation of organic matter that might have been generated during the first burial cycle in relation to the Variscan deformation phase. One sample in the Turnhout borehole yielded a very high crystallization temperature of 216 ± 6 °C and is interpreted to have crystallized during the first Upper Carboniferous burial cycle.

In the three boreholes studied also calcites were encountered that crystallized at lower temperatures and also later in the burial history. Most of the time these veins do not possess cleavage twins. They were dated as Late Meso- and Early Cenozoic. This might indicate that two additional deformation events have to be taken into account for the Campine Basin. In contrast with Poederlee where saddle dolomites associated with pyrite were reported in literature as being the product of Fe-rich hot saline fluids formed at maximum burial during the Sudetic phase, the coarse crystalline non-ferroan dolomites analyzed in the Turnhout borehole display lower temperatures varying around 80 °C. An exact timing of this vein development in Turnhout was unfortunately not possible, but it reflects another dolomitization pulse than the one reported in literature from Poederlee. Overall the signatures of the open veins studied in Poederlee, Heibaart and Turnhout display many similarities, and open veins seem to have formed during uplift and/or renewed burial in the Late Meso- and/to Early Cenozoic. Thus for exploration and production purposes with respect to Lower Carboniferous geothermal reservoirs in the Campine Basin (Belgium) one needs to take the Cretaceous – Paleocene tectonic stress field into account to predict which fractures might still be open.

Funding

VITO is thanked for funding the PhD grant of Eva van der Voet. Funding of the analysis relied on KU Leuven research resources.

CRediT authorship contribution statement

Rudy Swennen: Conceptualization, Validation, Investigation, Resources, Data curtion, Writing – original draft, Visualization, Supervision, Project administration, Funding acquisition. **Eva van der Voet:** Investigation, Writing – review & editing, Visualization. **Wei Wei:** Writing – review & editing, Visualization. **Philippe Muchez:** Conceptualization, Validation, Writing – review & editing, Funding acquisition.

Declaration of Competing Interest

The authors declare that they have no known competing financial interests or personal relationships that could have appeared to influence the work reported in this paper.

Acknowledgements

The authors like to thank the Belgian Geological Survey for providing the studied samples. Herman Nijs is thanked for the preparation of excellent thick- and thin-sections. Stable isotope analyses were carried out under supervision of Prof. M. Joachimsky (Erlangen, Germany), while the clumped isotopes were supervised by Dr. L. Rinyu (Debrecen, Hungary). We thank Dr. A. Gerdes (Frankfurt, Germany) for carrying out the U/Pb age dating.

Supplementary materials

Supplementary material associated with this article can be found, in the online version, at doi:10.1016/j.geothermics.2021.102147.

References

Berckmans, A., Vandenberghe, N., 1998. Use and potential of geothermal energy in Belgium. Geothermics 27, 235–242.

Bergerat, F., Vandycke, S., 1994. Cretaceous and Tertiary fault systems in the Boulonnais and Kent areas: Paleostress analysis and geodynamical implications. J. Geol. Soc. Lond. 151, 439–448.

Bernasconi, S.M., Daeron, M., Bergmann, K.D., Bonifacie, M., Meckler, A.N., Affek, H.P., Anderson, N., Bajnai, D., Barkan, E., Beverly, E., Blamart, D., Burgener, L., Calmels, D., Chaduteau, C., Clog, M., Davidheiser-Kroll, B., Davies, A., Dux, F., Eiler, J., Elliott, B., Fetrow, A.C., Fiebig, J., Goldberg, S., Hermoso, M., Huntington, K.W., Hyland, E., Ingalls, M., Jaggi, M., John, C.M., Jost, A. B., Katz, S., Kelson, J., Kluge, T., Kocken, I.J., Laskar, A., Leutert, T.J., Liang, D., Lucarelli, J., Mackey, T. J., Mangenot, X., Meinicke, N., Modestou, S.E., Muller, I.A., Murray, S., Neary, A., Packard, N., Passey, B.H., Pelletier, E., Petersen, S., Piasecki, A., Schauer, A,. Snell, K.E., Swart, P.K., Tripati, A., Upadhyay, D., Vennemann, T., Winkelstern, I., Yarian, D., Yoshida, N., Zhang, N., Ziegler, M., 2020, InterCarb: A community effort to improve inter-laboratory standardization of the carbonate clumped isotope thermometer using carbonate standards. Geochem. Geophys. Geosyst. (in press), https://doi.org/10.1002/essoar.10504430.4.

Bernasconi, S.M., Müller, I.A., Bergmann, K.D., Breitenbach, S.F.M., Fernandez, A., Hodell, D.A., Jaggi, M., Meckler, A.N., Millan, I., Ziegler, M., 2018. Reducing uncertainties in carbonate clumped isotope analysis through consistent carbonate-based standardization. Geochem. Geophys. Geosyst. 19, 2895–2914.

Bertier, P., Swennen, R., Lagrou, D., Laenen, B., Dreesen, R., 2008. Contrasting diagenesis of the Westphalian C & D sandstones in the Campine Basin (NE-Belgium). Sedimentology 55, 1375–1418.

Bless, M.J.M., Boonen, P., Dusar, M., Soille, P., 1981. Microfossils and depositional environment of Late Dinantian carbonates at Heibaart (Northern Belgium). Ann. Soc. Geol. Belg. 104, 135–165.

Bless, M.J.M., Bouckaert, J. and Paproth, E., 1983. Recent exploration in Pre-Permian rocks around the Brabant Massif in Belgium, The Netherlands and the Federal Republic of Germany. In: J. P. H. Kaasschieter & T. J. A. Reijers (eds.): Petroleum Geology of the Southeastern North Sea and the Adjacent Onshore Areas (The Hague, 1982). Geol. Mijnbouw 62, 51–62.

Böker, U., Dijksman, B., van den Graaff, E., 2012. Winterton area Dinantian prospectivity review, technical summary and concepts for reservoir models, Project G977. PanTerra Geoconsul. (Leiderdorp).

Bos, S., Laenen, B., 2017. Development of the first deep geothermal doublet in the Campine Basin of Belgium. Eur. Geol. 43, 16–20.

Brand, U., 2006. The oxygen and carbon isotope composition of Carboniferous fossil components: sea-water effects. Sedimentology 29, 139–147.

Broothaers, M., Bos, S., Lagrou, D., Harcouët-Menou, V., Laenen, B., 2019. Lower Carboniferous limestone reservoir in northern Belgium: structural insights from the Balmatt project in Mol. European Geothermal Congress 2019. The Hague, The Netherlands.

Burisch, M., Gerdes, A., Walter, B.F., Neumann, U., Fettel, M., Markl, G., 2017. Methane and the origin of five-element veins: Mineralogy, age, fluid inclusion chemistry and ore forming processes in the Odenwald, SW Germany. Ore Geol. Rev. 81, 42–61.

Dreesen, R., Bouckaert, J., Dusar, M., Soille, J., Vandenberghe, N., 1987. Subsurface Structural Analysis of the Late-Dinantian Carbonate Shelf at the Northern Flank of the Brabant Massif (Campine Basin, N-Belgium), 21. Toelicht. Verhand. Geologische en Mijnkaarten van België, p. 37.

Dreesen, R., Laenen, B., 2010. Technology Watch: geothermie en het potentieel in Vlaanderen. Eindrapport. Studie uitgevoerd in opdracht van de Vlaamse overheid. Departement LNE, Afdeling ALBON, p. 64. Vito-2010/SCT/R/001.

Duperret, A., Vandycke, S., Mortimore, R.N., Genter, A., 2012. How plate tectonics is recorded in chalk deposits along the eastern English Channel in Normandy (France) and Sussex (UK). Tectonophysics 581, 163–181.

Emrich, K, Ehhalt, D.H., Vogel, J.C., 1970. Carbon isotope fractionation during the precipitation of calcium carbonate. Earth Planet. Sci. Lett. 8, 363–371.

Gerdes, A., Zeh, A., 2006. Combined U–Pb and Hf isotope LA-(MC-)ICP-MS analyses of detrital zircons: Comparison with SHRIMP and new constraints for the provenance and age of an Armorican metasediment in Central Germany. Earth Planet. Sci. Lett. 249, 47–61. https://doi.org/10.1016/j.epsl.2006.06.039.

Gerdes, A., Zeh, A., 2009. Zircon formation versus zircon alteration - New insights from combined U–Pb and Lu–Hf in-situ LA-ICP-MS analyses, and consequences for the interpretation of Archean zircon from the Central Zone of the Limpopo Belt. Chem. Geol. 261, 230–243. https://doi.org/10.1016/j.chemgeo.2008.03.005.

Godeau, N. (2018) Développement et application de la méthode Uranium-Plomb à la datation des carbonates diagénétiques dans les réservoirs pétroliers, et apport à la reconstruction temporelle de l'évolution des propriétés réservoir. Ph.D. Aix-Marseille (France).

Grosjean, A., 1954. Mésures de temperatures aux profondeurs de 2185 et 2225 m dans le sondage de Turnhout (Campine Belge). Bull. Soc. Géol. Belgique 63, 193–201.

Gulinck, M., 1956. Caractéristiques hydrogéologiques du sondage de Turnhout, Communication de l'Observatoire Royal de Belgique, 108. Sér. Géophys. 37, 1–6.

Harings, M.J., 2014. CAL-GT-01 - Implications for the distribution of the early namurian geverik member in the Netherlands. Ext. Abstr. EAGE 2014.

Helsen, S., Langenaeker, V., 1999. Burial history and coalification modelling of Westphalian strata in the eastern Campine Basin (Northern Belgium). Geol. Surv. Bel., Prof. Paper 289.

Irwin, H., Curtis, C., Coleman, M., 1977. Isotopic evidence for source of diagenetic carbonates formed during burial of organic-rich sediments. Nature 269, 209–213.

Jaarsma, B., Brolsma, M.J., Hoetz, G., Lutgert, J.E., 2013. Exploring Dinantian carbonates in the SNS – new data offering new insights. In: 75th EAGE Conference and Exhibition incorporating SPE EUROPEC, 10–13 June, London, UK. EAGE (London).

John, C., Bowen, D., 2016. Community software for challenging isotope analysis: First applications of 'Easotope' to clumped isotopes. Rapid Commun. Mass Spectrom. 30, 2285–2300.

Kombrink, H., 2008. The Carboniferous of the Netherlands and surrounding areas; a basin analysis. Geol. Ultraiectina, Mededeling. Fac. Geowetenschappen 294, 184. Universiteit Utrecht (Utrecht).

Laenen, B., Van Tongeren, P., Dreesen, R., Dusar, M., 2004. Carbon dioxide sequestration in the Campine Basin and the adjacent Roer valley Graben (north Belgium): an inventory. Geol. Soc., London, Spec. Publ. 233, 193–210.

Land, L.S., 1983. The application of stable isotopes to studies of the origin of dolomite and to problems of diagenesis in clastic sediments. In: Arthur, M. A. (ed.) Stable isotopes in sedimentary geology. Society of Economic Paleontologists and Mineralogists Special Publication, 10. Short Course, pp. 4.1–4.22.

Langenaeker, V., 2000. The Campine Basin: Stratigraphy, Structural Geology, Coalification and Hydrocarbon Potential for the Devonian to Jurassic (Ph.D. thesis). KU Leuven.

Ludwig, K.R., 2009. Isoplot/Ex Ver 3.71: A Geochronological Toolkit for Microsoft Excel. Berkeley Geochronology Center Special Publications.

McCann, T., 2008. The Geology of Central Europe. Volume 1: Precambrian and Palaeozoic. Geological Society, London.

Muchez, Ph., Conil, R., Viaene, W., Bouckaert, J., Poty, E., 1987a. Sedimentology and biostratigraphy of the Visean carbonates of the Heibaart (DzH1) borehole (Northern Belgium). Annal. Soc. Géol. Bel. 110, 199–208.

Muchez, Ph., Fein, U.F., Van den Broeck, K., Vandecasteele, C., 1994a. Lithological influence on the composition of vein cements in the Carboniferous of the Campine Basin (northern Belgium). Eur. J. Mineral. 6, 985–994.

Muchez, Ph., Langenaeker, V., 1993. Middle Devonian to Dinantian sedimentation in the Campine Basin (northern Belgium): its relation to Variscan tectonism. Spec. Publ. Int. Assoc. Sedimentol. 20, 171–181.

Muchez, Ph., Marshall, J., Touret, J.L.R., Viaene, W., 1994b. Origin and migration of palaeofluids in the Visean of the Campine Basin, northern Belgium. Sedimentology 41, 133–145.

Muchez, P., Peeters, C., Keppens, E., Viaene, W., 1993. Stable isotopic composition of paleosols in the lower Visean of eastern Belgium - evidence of evaporation and soil-gas CO_2. Chem. Geol. 106 (3), 389–396.

Muchez, Ph., Viaene, W., Bouckaert, J., Conil, R., Dusar, M., Poty, E., Soille, P., Vandenberghe, N., 1990. The occurrence of a microbial buildup at Poederlee (Campine Basin, Belgium): biostratigraphy, sedimentology, early diagenesis and significance for early Warnantian paleogeography. Annal. Soc. Géol. Bel. 113, 329–339.

Muchez, Ph., Viaene, W., Keppens, E., Marshal, J.D., Vandenberghe, N., 1991a. Vein cements and the geochemical evolution of subsurface fluids in the Visean of the Campine Basin (Poederlee borehole, Belgium). J. Geol. Soc., Lond. 148, 1005–1117.

Muchez, Ph., Viaene, W., Marshall, J.D., 1991b. Origin of shallow burial cements in the late viséan of the Campine Basin, Belgium. Sediment. Geol. 73, 257–271.

Muchez, Ph., Viaene, W., Wolf, M., Bouckaert, J., 1987b. Sedimentology, coalification pattern and paleogeography of the Campine-Brabant Basin during the Visean. Geol. Mijnbouw 66, 313–326.

Nelson, R.A., 1985. Geological Analysis of Naturally Fractured Reservoirs. Gulf Publishing Company, Houston, Texas.

Poty, E., 2014. Report on Cuttings from the CAL-GT-01 Borehole. Unpublished report EBN BV.

O'Neil, J R, Clayton, R.N., Mayeda, T.K., 1969. Oxygen isotope fractionation in divalent metal carbonates. J. Chem. Phys. 51, 5547–5558.

Reijmer, J.J.G., ten Veen, J.H., Jaarsma, B., Boots, R., 2017. Seismic stratigraphy of Dinantian carbonates in the southern Netherlands and northern Belgium. Neth. J. Geosci.- Geol. Mijnb. 96, 353–379. https://doi.org/10.1017/njg.2017.33.

Reith, D., Godderij, R., Jaarsma, B., Bertotti, G., Heijnen, L., 2019. Dynamic simulation of a geothermal reservoir: case study of the dinantian carbonates encountered in the Californië geothermal wells. In: European Geothermal Congress proceedings, Den Haag, The Netherlands, 11-14 June 2019. Limburg, NL, pp. 1–18.

Ring, U., Gerdes, A., 2016. Kinematics of the Alpenrhein-Bodensee graben system in the Central Alps: Oligocene/Miocene transtension due to formation of the Western Alps arc. Tectonics 35, 1367–1391. https://doi.org/10.1002/2015TC004085.

Rossa, H.G., 1986. Upper Cretaceous and Tertiary inversion tectonics in the western part of the Rhenish-Westphalian Coal District (FRG) and in the Campine area (N Belgium). Annal. Soc. Géol. Bel. 109, 367–410.

Savard, M., Bourque, P.-A., 1989. Diagenetic evolution of a late silurian reef platform, Gaspé Basin, Quebec, based on cathodoluminescence petrography. Can. J. Earth Sci. 26, 791–806.

Ten Have, T., Heijnen, W., 1985. Cathodoluminescence activation and zonation in carbonate rocks: an experimental approach. Geol. Mijnbouw 64, 297–310.

TOTAL E & P UK, 2007. A regional review of the Dinantian carbonate play: Southern North Sea and onshore UK. Total E & P UK.

Vandenberghe, N., Bouckaert, J., 1980. Geologische beschouwingen van geothermische mogelijkheden in Noord-België. Belg. Geol. Dienst Prof. Paper 1980 168, 1–21.

Vandenberghe, N., De Craen, M., Beerten, K., 2014. Geological framework of the Campine Basin Geological setting, tectonics, sedimentary sequences. External report SCK•CEN-ER-262 14/MDC/P-43, 112pp.

Vandenberghe, N., Dusar, M., Boonen, P., Lie, S.F., Voets, R., Bouckaert, J., 2000. The Merksplas-Beerse geothermal well (17W265) and the Dinantian reservoir. Geol. Bel. 3, 349–367.

Vandenberghe, N., Van Simaeys, S., Steurbaut, E., Jagt, J.W.M., Felder, P.J., 2004. Stratigraphic architecture of the Upper Cretaceous and Cenozoic along the southern border of the North Sea Basin in Belgium. Neth. J. Geosci./Geol. Mijnbouw 83 (3), 155–171.

Van der Voet, E., Muchez, Ph., Laenen, B., Weltje, G.J., Lagrou, D., Swennen, R., 2020a. Characterizing carbonate reservoir fracturing from borehole data – A case study of the Viséan in northern Belgium. Mar. Pet. Geol. 111, 375–389.

Van der Voet, E., Laenen, B., Rombaut, B., Kourta, M., Swennen, R., 2020b. Fracture characteristics of lower carboniferous carbonates in northern Belgium based on FMI log analyses. Neth. J. Geosci. 99, E8.

Van der Voet, E., Laenen, B., Muchez, P., Lagrou, D., Claes, H., Verbiest, M. and Swennen, R., in preparation. Controls of dolomitization and bed thickness on fracture intensity in Lower Carboniferous carbonates in southern Belgium. Manuscript submitted for publication.

Vandycke, S., 2002. Palaeostress records in Cretaceous formations in NW Europe: synsedimentary strike-slip and extensional tectonics events. Relationships with Cretaceous-Tertiary inversion tectonics. Tectonophysics 357, 119–136, 1-4.

Vandycke, S., Bergerat, F., 1989. Analyse microtectonique des déformations cassantes dans le Bassin de Mons. Reconstitution des paléo-champs de contrainte au Crétacé-Tertiaire. Annal. Soc. Géol. Bel. 112, 479–487.

Vandycke, S., Bergerat, F., 1992. Tectonique de failles et paléocontraintes dans les formations crétacées du Boulonnais (N France). Bull. Soc. Géol. France 163, 553–560.

Vandycke, S., Bergerat, F., 2001. Brittle structures tectonic structures and palaeostress analysis in the Isle of Wight, Wessex Basin, Southern U.K. J. Struct. Geol. 23, 393–406.

Vandycke, S., Bergerat, F., Dupuis, C., 1991. Meso-Cenozoic faulting and inferred paleostresses of the Mons basin (Belgium). Tectonophysics 192, 261–271.
Van Hulten, F.F.N., Poty, E., 2008. Geological factors controlling Early Carboniferous carbonate platform development in the Netherlands. Geol. J. 43, 175–196.
Van Keer, I., Ondrak, R., Muchez, Ph., Bayer, U., Dusar, M., Viaene, W., 1998. Burial history and thermal evolution of Westphalian coal-bearing strata in the Campine Basin (NE Belgium). Geol. Mijnbouw 76, 301–310.
Van Wijhe, D.H., 1987. Structural evolution of inverted basins in the Dutch offshore. Tectonophysics 137, 171–219.
Warr, O., Giunta, T., Onstott, T.C., Kieft, T.L., Harris, R.L., Nisson, D.M., Lollar, B.S., 2021. The role of low-temperature ^{18}O exchange in the isotopic evolution of deep subsurface fluids. Chem. Geol. 561, 26. doi.org/10.1016/j.chemgeo.2020.120027.
Walkden, G.M., Berry, J.R., 1984. Syntaxial overgrowths in muddy crinoidal limestones: cathodoluminescence sheds new light on an old problem. Sedimentology 38, 643–670.
Warren, J.E., Root, P.J., 1963. The behaviour of naturally fractured reservoirs. SPE J. 426, 245–255. https://doi.org/10.2118/426-PA. -PA.
Noordzee, W., 2006. Promote Licence P1252, Two Year Report, Blocks: 53/15b, 53/19, 53/20, 54/11 and 54/16. Wintershall Noordzee BV (Rijswijk).
Ziegler, P.A., 1990. Geological Atlas of Western and Central Europe (2nd edition). The Hague: Shell Internationale Petroleum Maatschappij B.V. Geological Society Publishing House, Bath.